



# Structure, variation, and assembly of the root-associated microbiomes of rice

Joseph Edwards<sup>a</sup>, Cameron Johnson<sup>a,1</sup>, Christian Santos-Medellín<sup>a,1</sup>, Eugene Lurie<sup>a,2</sup>, Natraj Kumar Podishetty<sup>b</sup>, Srijak Bhatnagar<sup>c</sup>, Jonathan A. Eisen<sup>c</sup>, and Venkatesan Sundaresan<sup>a,b,3</sup>

Departments of <sup>a</sup>Plant Biology, <sup>b</sup>Plant Sciences, and <sup>c</sup>Medical Microbiology and Immunology, University of California, Davis, CA 95616

Edited by Jeffery L. Dangl, Howard Hughes Medical Institute and The University of North Carolina at Chapel Hill, Chapel Hill, NC, and approved December 22, 2014 (received for review July 31, 2014)

Plants depend upon beneficial interactions between roots and microbes for nutrient availability, growth promotion, and disease suppression. High-throughput sequencing approaches have provided recent insights into root microbiomes, but our current understanding is still limited relative to animal microbiomes. Here we present a detailed characterization of the root-associated microbiomes of the crop plant rice by deep sequencing, using plants grown under controlled conditions as well as field cultivation at multiple sites. The spatial resolution of the study distinguished three root-associated compartments, the endosphere (root interior), rhizoplane (root surface), and rhizosphere (soil close to the root surface), each of which was found to harbor a distinct microbiome. Under controlled greenhouse conditions, microbiome composition varied with soil source and genotype. In field conditions, geographical location and cultivation practice, namely organic vs. conventional, were factors contributing to microbiome variation. Rice cultivation is a major source of global methane emissions, and methanogenic archaea could be detected in all spatial compartments of field-grown rice. The depth and scale of this study were used to build coabundance networks that revealed potential microbial consortia, some of which were involved in methane cycling. Dynamic changes observed during microbiome acquisition, as well as steady-state compositions of spatial compartments, support a multistep model for root microbiome assembly from soil wherein the rhizoplane plays a selective gating role. Similarities in the distribution of phyla in the root microbiomes of rice and other plants suggest that conclusions derived from this study might be generally applicable to land plants.

microbiomes | rice | soil microbial communities | methane cycling | microbiome assembly

Land plants grow in soil, placing them in direct proximity to a high abundance of microbial diversity (1). Plants and microbes have both adapted to use their close association for their mutual benefit. Critical nutrients are converted to more usable forms by microbes before assimilation by plants (2–4). In turn, bacteria in the rhizosphere receive carbon metabolites from the plant through root exudates (5). Beneficial soil microbes also contribute to pathogen resistance, water retention, and synthesis of growth-promoting hormones (6–8).

Recent studies have used high-throughput sequencing to provide new insights into the bacterial composition and organization of different plant microbiomes, including *Arabidopsis*, *Populus*, and maize (9–14). Detailed characterization of the core root microbiome of *Arabidopsis* (9–11) showed that the dominant phyla inside the root (the endosphere) are much less diverse than the phyla in the soil around the root (the rhizosphere), and a potential core root microbiome could be identified. In *Arabidopsis*, the endophytic microbiome exhibits some genotype-dependent variation within the species and an increased variation when other related species are examined (9–11). A recent study in maize examined microbiome variation across many different inbred lines at different sites and found a large variation arising from geographical location between three different states in the United States and a relatively smaller dependence on the genotype (12). Although the

microbiomes examined in the maize study consisted of combined rhizospheric and endospheric microbes (12), a study in poplar found that the variation between locations in two different states affected both rhizospheric and endospheric microbes (14).

These studies have opened the way toward a new understanding of the composition and structure of plant microbiomes and the factors that affect them. However, this understanding is still at the initial stages, and several key questions are as yet unanswered. One such question regards the mechanism of microbiome acquisition and assembly in plants. Unlike animals, where the gut microbiome is assembled internally and is transmissible through birth (15, 16), the root microbiome is predominantly assembled from the external microbes in the soil. Based on the composition of the endospheric and rhizospheric microbiomes, it has been proposed that plants might assemble their microbiomes in two steps, with the first step involving a general recruitment to the vicinity of the root and a second step for entry inside the root that involves species-specific genetic factors (7). Although this is a plausible hypothesis, direct support for this model through detailed dynamic studies has not yet been provided. Additionally, the role of the root surface or rhizoplane, which forms the critical interface between plants and soil, remains poorly understood, and the microbial composition of the rhizoplane in relation to those of the rhizosphere and endosphere is unknown.

## Significance

Land plants continuously contact beneficial, commensal, and pathogenic microbes in soil via their roots. There is limited knowledge as to how the totality of root-associated microbes (i.e., the microbiome) is shaped by various factors or its pattern of acquisition in the root. Using rice as a model, we show that there exist three different root niches hosting different microbial communities of eubacteria and methanogenic archaea. These microbial communities are affected by geographical location, soil source, host genotype, and cultivation practice. Dynamics of the colonization pattern for the root-associated microbiome across the three root niches provide evidence for rapid acquisition of root-associated microbiomes from soil, and support a multistep model wherein each root niche plays a selective role in microbiome assembly.

Author contributions: J.E., C.J., C.S.-M., and V.S. designed research; J.E., C.S.-M., E.L., and N.K.P. performed research; S.B. and J.A.E. contributed new reagents/analytic tools; J.E. analyzed data; and J.E. and V.S. wrote the paper.

The authors declare no conflict of interest.

This article is a PNAS Direct Submission.

Freely available online through the PNAS open access option.

Data deposition: The sequence reported in this paper has been deposited in the National Center for Biotechnology Information Short Read Archive (accession no. [SRP044745](#)).

See Commentary on page 2299.

<sup>1</sup>C.J. and C.S.-M. contributed equally to this work.

<sup>2</sup>Present address: Department of Molecular and Human Genetics, Baylor College of Medicine, Houston, TX 77030.

<sup>3</sup>To whom correspondence should be addressed. Email: [sundar@ucdavis.edu](mailto:sundar@ucdavis.edu).

This article contains supporting information online at [www.pnas.org/lookup/suppl/doi:10.1073/pnas.1414592112/-DCSupplemental](http://www.pnas.org/lookup/suppl/doi:10.1073/pnas.1414592112/-DCSupplemental).

To address some of these questions, we have undertaken an exhaustive characterization of the root-associated microbiome of rice. Rice is a major crop plant and a staple food for half of the world's population. Metagenomic and proteomic approaches have been used to identify different microbial genes present in the rice microbiome (17, 18), but an extensive characterization of microbiome composition and variation has not been performed. Rice cultivation also contributes to global methane, accounting for an estimated 10–20% of anthropogenic emissions, due to the growth of methanogenic archaea in the vicinity of rice roots (19). Here we have used deep sequencing of microbial 16S rRNA genes to detect over 250,000 operational taxonomic units (OTUs), with a structural resolution of three distinct compartments (rhizosphere, rhizoplane, and endosphere) and extending over multiple factors contributing to variation, both under controlled greenhouse conditions as well as different field environments. The large datasets from the different conditions sampled in this study were used for identification of putative microbial consortia involved in processes such as methane cycling. Through dynamic studies of the microbiome composition, we provide insights into the process of root microbiome assembly.

## Results

**Root-Associated Microbiomes Form Three Spatially Separable Compartments Exhibiting Distinct and Overlapping Microbial Communities.** Sterilized rice seeds were germinated and grown under controlled greenhouse conditions in soil collected from three rice fields across the Central Valley of California (*SI Appendix*, Fig. S1). We analyzed the bacterial and archaeal microbiomes from three separate rhizocompartments: the rhizosphere, rhizoplane, and endosphere (Fig. 1A). Because the root microbiome has been shown to correlate with the developmental stage of the plant (10), the root-associated microbial communities were sampled at 42 d (6 wk), when rice plants from all genotypes were well-established in the soil but still in their vegetative phase of growth. For our study, the rhizosphere compartment was com-

posed of ~1 mm of soil tightly adhering to the root surface that is not easily shaken from the root (*SI Appendix*, Fig. S2). The rhizoplane compartment microbiome was derived from the suite of microbes on the root surface that cannot be removed by washing in buffer but is removed by sonication (*SI Appendix*, Materials and Methods). The endosphere compartment microbiome, composed of the microbes inhabiting the interior of the root, was isolated from the same roots left after sonication. Unplanted soil pots were used as a control to differentiate plant effects from general edaphic factors.

The V4-V5 region of the 16S rRNA gene was amplified using PCR and sequenced using the Illumina MiSeq platform. A total of 10,554,651 high-quality sequences was obtained with a median read count per sample of 51,970 (range: 2,958–203,371; *Dataset S2*). The high-quality reads were clustered using >97% sequence identity into 101,112 microbial OTUs. Low-abundance OTUs (<5 total counts) were discarded, resulting in 27,147 OTUs. The resulting OTU counts in each library were normalized using the trimmed mean of M values method. This method was chosen due to its sensitivity for detecting differentially abundant taxa compared with traditional microbiome normalization techniques such as rarefaction and relative abundance (20). Measures of within-sample diversity ( $\alpha$ -diversity) revealed a diversity gradient from the endosphere to the rhizosphere (Fig. 1B and *Dataset S4*). Endosphere communities had the lowest  $\alpha$ -diversity and the rhizosphere had the highest  $\alpha$ -diversity. The mean  $\alpha$ -diversity was higher in the rhizosphere than bulk soil; however, the difference in  $\alpha$ -diversity between these two compartments cannot be considered as statistically significant (Wilcoxon test; *Dataset S4*).

Unconstrained principal coordinate analyses (PCoAs) of weighted and unweighted UniFrac distances were performed to investigate patterns of separation between microbial communities (*SI Appendix*, Materials and Methods). The UniFrac distance is based on taxonomic relatedness, where the weighted UniFrac (WUF) metric takes abundance of taxa into consideration whereas the unweighted UniFrac (UUF) does not and is thus more sensitive to rare taxa. In both the WUF and UUF PCoAs, the rhizocompartments separate across the first principal coordinate, indicating that the largest source of variation in root-associated microbial communities is proximity to the root (Fig. 1C, WUF and *SI Appendix*, Fig. S4, UUF). Moreover, the pattern of separation is consistent with a gradient of microbial populations from the exterior of the root, across the rhizoplane, and into the interior of the root. Permutational multivariate analysis of variance (PERMANOVA) corroborates that rhizospheric compartmentalization comprises the largest source of variation within the microbiome data when using a WUF distance metric (46.62%,  $P < 0.001$ ; *Dataset S5A*). PERMANOVA using a UUF distance, however, describes rhizospheric compartmentalization as having the second largest source of variation behind soil type (18.07%,  $P < 0.001$ ; *Dataset S5H*). In addition to PERMANOVA, we also performed partial canonical analysis of principal coordinates (CAP) on both the WUF and UUF metrics to quantify the variance attributable to each experimental variable (*SI Appendix*, Materials and Methods). This technique differs from unconstrained PCoA in that technical factors can be controlled for in the analysis and the analysis can be constrained to any factor of interest to better understand the quantitative impact of the factor on the microbial composition. Using this technique to control for soil type, cultivar, and technical factors (biological replicate, sequencing batch, and planting container), we found that in agreement with the PERMANOVA results, microbial communities vary significantly between rhizocompartments (34.2% of variance,  $P = 0.005$ , WUF, *SI Appendix*, Fig. S5A and 22.6% of variance,  $P = 0.005$ , UUF, *SI Appendix*, Fig. S5C).

There are notable differences in the proportions of various phyla across the compartments that are consistent across every tested soil (Fig. 1D). The endosphere has a significantly greater proportion of Proteobacteria and Spirochaetes than the rhizosphere or bulk soil, whereas Acidobacteria, Planctomycetes, and Gemmatimonadetes are mostly depleted in the endosphere

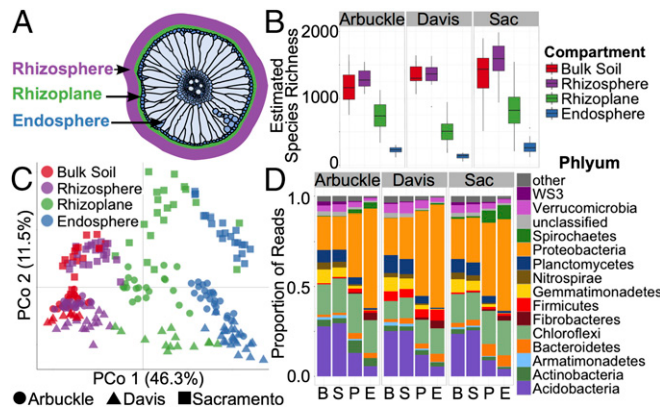


**Fig. 1.** Root-associated microbial communities are separable by rhizo-compartment and soil type. (A) A representation of a rice root cross-section depicting the locations of the microbial communities sampled. (B) Within-sample diversity ( $\alpha$ -diversity) measurements between rhizospheric compartments indicate a decreasing gradient in microbial diversity from the rhizosphere to the endosphere independent of soil type. Estimated species richness was calculated as  $e^{Shannon\_entropy}$ . The horizontal bars within boxes represent median. The tops and bottoms of boxes represent 75th and 25th quartiles, respectively. The upper and lower whiskers extend 1.5x the interquartile range from the upper edge and lower edge of the box, respectively. All outliers are plotted as individual points. (C) PCoA using the WUF metric indicates that the largest separation between microbial communities is spatial proximity to the root (PCo 1) and the second largest source of variation is soil type (PCo 2). (D) Histograms of phyla abundances in each compartment and soil. B, bulk soil; E, endosphere; P, rhizoplane; S, rhizosphere; Sac, Sacramento.

compared with the bulk soil or rhizosphere (Wilcoxon test; **Dataset S6**). The reduction in relative abundance of these phyla across the compartments is consistent with the observation that microbial diversity decreases from the rhizosphere to the endosphere.

**Association of Significantly Enriched OTUs with Different Rhizocompartments.** To identify OTUs that are correlated with community separation between the compartments, we conducted differential OTU abundance analysis by fitting a generalized linear model with a negative binomial distribution to normalized values for each of the 27,147 OTUs in the greenhouse experiment and testing for differential abundance using a likelihood ratio test (**Dataset S7**). Using OTU counts from unplanted soil as a control and an adjusted *P* value cutoff of 0.01, there were 578 OTUs that were significantly enriched in at least one compartment. The rhizosphere was the most similar to bulk soil, as indicated by the “tail” in the MA plot (Fig. 2A); however, an enrichment effect in the rhizosphere is implied by the high ratio of statistically significant enriched OTUs compared with depleted OTUs (152 vs. 17). In comparison, the rhizoplane enriches for many OTUs while simultaneously depleting a larger proportion of OTUs (422 vs. 730). The endosphere is the most exclusive compartment, enriching for 394 OTUs while depleting 1,961 OTUs (Fig. 2A).

There were noteworthy overlaps in differentially abundant OTUs between the compartments (Fig. 2B and C). The OTUs enriched in the rhizosphere are very successful at colonizing the root, as 119 out of the 152 OTUs enriched in the rhizosphere are also enriched in either the rhizoplane or endosphere communities or both (Fig. 2B). There was a set of 96 OTUs mainly consisting of Bacteroidetes, Firmicutes, Chloroflexi, and Betaproteobacteria that were differentially enriched in all rhizocompartments compared with bulk soil (*SI Appendix*, Fig. S6A). The Betaproteobacterial OTUs that are enriched in every rhizocompartment correspond mainly to *Rhodocyclaceae* and *Comamonadaceae* (*SI*

*Appendix*, Fig. S6B). OTUs belonging to the genus *Pleomorphomonas* are also enriched in all of the rhizocompartments (**Dataset S7**). Some members within the *Pleomorphomonas* genus are capable of nitrogen fixation (21–23). The rhizoplane and endosphere were the most similar rhizocompartments, sharing 271 enriched OTUs. Most of the OTUs enriched between the rhizoplane and endosphere compartments belonged to Alpha-, Beta-, and Deltaproteobacterial classes, Chloroflexi, and Bacteroidetes. Not surprisingly, a subset of the OTUs enriched in the endosphere and rhizoplane belong to Fibrobacteres and Spirochaetes, phyla that are associated with cellulose degradation (24, 25).

It was possible to quantify exclusionary effects of each compartment by analyzing OTU abundance relative to bulk soil (Fig. 2A). The rhizosphere had a small effect on excluding microbes, as only 17 OTUs were significantly depleted compared with bulk soil. These OTUs were mainly in the Proteobacteria and Acidobacteria phyla (*SI Appendix*, Fig. S7). Many more OTUs were reduced in relative abundance in the rhizoplane (730 OTUs, mainly Acidobacteria and Planctomycetes; *SI Appendix*, Fig. S7), and even more OTUs (1,961 OTUs, mainly Acidobacteria, Planctomycetes, Chloroflexi, and Verrucomicrobia; *SI Appendix*, Fig. S7) were reduced in the endosphere. There are considerable overlaps in the OTUs that are excluded from each compartment (Fig. 2C). Nearly all of the OTUs depleted from the rhizosphere are also depleted in the rhizoplane and endosphere communities. The rhizoplane shares 713 of the 1,961 OTUs that are significantly depleted from the endosphere. These results indicate that plant-controlled changes in the rhizospheric soil are the first level of exclusion of microbial colonization of the root and that selectivity at the rhizoplane might act effectively as a gate for controlling entry of the microbes into the root endosphere. Similar patterns were present when each soil type was analyzed separately (*SI Appendix*, Fig. S8 B–G).

**Microbial Communities Colonizing Rhizocompartments Vary by Soil Type.** To investigate how soil variation might affect the root microbiome, plants were grown in soil collected from rice fields at three locations from across the California Sacramento Valley: Davis, Sacramento, and Arbuckle (*SI Appendix*, Fig. S1). Both the Arbuckle and Sacramento fields primarily grow rice and were drained 3 wk before soil collection. The Davis site had previously grown rice for several years; however, it was not cultivated the year before soil collection. By growing the plants in controlled greenhouse conditions, we aimed to control for climatic variations between the sites and identify only changes attributable to the different soils.

$\alpha$ -Diversity measurements comparing microbial communities between each soil type revealed a small but significant difference in diversity (1.54% variance explained,  $P = 2.54\text{E-}5$ , ANOVA; **Dataset S3**). The two cultivated fields (Arbuckle and Sacramento) had significantly higher diversities in the rhizoplane and endosphere microbial communities than the uncultivated Davis field (Fig. 1B and **Dataset S4**). PCoA shows that rhizosphere samples from plants grown in the distinct soils separate along the second axis and that the separation pattern manifests in every compartment (Fig. 1C, WUF and *SI Appendix*, Fig. S4, UUF). The Arbuckle and Davis rhizosphere microbiomes were most similar to each other despite being the most geographically separated. PERMANOVA using the WUF distance supports the PCoA results that the soil effect describes the second largest source of variation in the tested factors of the experiment (**Dataset S5A**). PERMANOVA using the UUF distance measure indicates that the soil effect has the largest source of variation in the factors tested (20.90%,  $P < 0.001$ ; **Dataset S5H**). CAP analysis constrained to soil type and controlling for rhizocompartment, cultivar, and technical factors agreed with the PERMANOVA result in that soil type explained the second largest source of variation in the microbial communities behind compartment when using the WUF metric (20.2%,  $P = 0.005$ ; *SI Appendix*, Fig. S5B) and the largest source of variation when

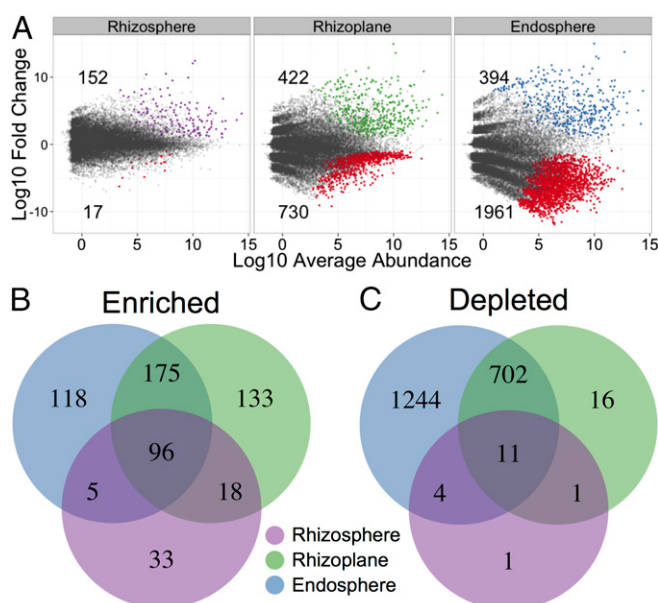


**Fig. 2.** Rhizocompartments are enriched and depleted for certain OTUs. (A) Enrichment and depletion of the 27,147 OTUs included in the greenhouse experiment for each rhizospheric compartment compared with bulk soil controls as determined by differential abundance analysis. Each point represents an individual OTU, and the position along the *y* axis represents the abundance fold change compared with bulk soil. (B) Numbers of differentially enriched OTUs between each compartment compared with bulk soil. (C) Numbers of differentially depleted OTUs between each compartment.

using the UUF metric (26.7%,  $P = 0.005$ ; *SI Appendix*, Fig. S5D). This discrepancy is likely due to differences between the WUF and UUF distance metric: Soil type might have more of an effect on frequency of rare taxa than abundant taxa, and thus the UUF metric has a larger effect size for soil type. Compartments of plants grown in distinct soils have commonalities in differentially abundant OTUs (Dataset S9), sharing 92 endosphere-enriched OTUs, 71 rhizoplane-enriched OTUs, and 10 rhizosphere OTUs (*SI Appendix*, Fig. S8 J, I, and H, respectively, and *SI Appendix*, Fig. S9). In agreement with the PCoA analysis, Davis and Arbuckle shared a significant overlap in OTUs enriched in the endosphere and rhizoplane ( $P = 2.22 \times 10^{-16}$  and  $7.86 \times 10^{-7}$ , respectively, hypergeometric test; *SI Appendix*, Fig. S8 I and J) but not the rhizosphere ( $P = 0.52$ , hypergeometric test; *SI Appendix*, Fig. S8H). The Sacramento soil did not share significant overlaps in compartment-enriched OTUs with the other sites.

The enrichment/depletion effects within each rhizosphere compartment vary by soil. Rhizosphere compartments of plants in Davis and Arbuckle soils exhibited higher enrichment/depletion ratios (72/3 and 53/17, respectively) than plants in Sacramento soil (78/116) (*SI Appendix*, Fig. S8A). The level of enrichment is similar between each soil in the rhizosphere; however, the depletion level is higher in Sacramento soil than in Arbuckle or Davis. Chemical analysis of the soils showed that the nutrient compositions of the soils did not show any exceptional trends (Dataset S7). The Davis and Arbuckle fields were similar in pH and nitrate, magnesium, and phosphorus content, whereas the Arbuckle and Sacramento fields were similar in potassium, calcium, and iron content. Taken together, these results indicate that each soil contains a different pool of microbes and that the plant is not restricted to specific OTUs but instead draws from available OTUs in the pool to organize its microbiome. Nevertheless, the distribution of phyla across the different compartments was similar for all three soil types (Fig. 1D), suggesting that the overall recruitment of OTUs is governed by a set of factors that result in a consistent representation of phyla independent of soil type.

**Microbial Communities in the Rhizocompartments Are Influenced by Rice Genotype.** To investigate the relationship between rice genotype and the root microbiome, domesticated rice varieties cultivated in widely separated growing regions were tested. Six cultivated rice varieties spanning two species within the *Oryza* genus were grown for 42 d in the greenhouse before sampling. Asian rice (*Oryza sativa*) cultivars M104, Nipponbare (both temperate *japonica* varieties), IR50, and 93-11 (both *indica* varieties) were grown alongside two cultivars of African cultivated rice *Oryza glaberrima*, TOG7102 (Glab B) and TOG7267 (Glab E). PERMANOVA indicated that rice genotype accounted for a significant amount of variation between microbial communities when using WUF (2.41% of the variance,  $P < 0.001$ ; Dataset S5A) and UUF (1.54% of the variance,  $P < 0.066$ ; Dataset S5H); however, visual representations for clustering patterns of the genotypes were not evident on the first two axes of unconstrained PCoA ordinations (*SI Appendix*, Fig. S10). We then used CAP analysis to quantify the effect of rice genotype on the microbial communities. By focusing on rice cultivar and controlling for compartment, soil type, and technical factors, we found that genotypic differences in rice have a significant effect on root-associated microbial communities (5.1%,  $P = 0.005$ , WUF, Fig. 3A and 3.1%,  $P = 0.005$ , UUF, *SI Appendix*, Fig. S11A). Ordination of the resulting CAP analysis revealed clustering patterns of the cultivars that are only partially consistent with genetic lineage for both the WUF and UUF metrics. The two *japonica* cultivars clustered together and the two *O. glaberrima* cultivars clustered together; however, the *indica* cultivars were split, with 93-11 clustering with the *O. glaberrima* cultivars and IR50 clustering with the *japonica* cultivars.

To analyze how the genotypic effect manifests in individual rhizocompartments, we separated the whole dataset to focus on each compartment individually and conducted CAP analysis controlling for soil type and technical factors. The rhizosphere

had the greatest genotypic effect on the microbiome (30.3%,  $P = 0.005$ , WUF, *SI Appendix*, Fig. S11B and 10.5%,  $P = 0.005$ , UUF, *SI Appendix*, Fig. S11E). The clustering patterns of the cultivars in the rhizosphere were similar to the clustering patterns exhibited when conducting CAP analysis on the whole data using all rhizocompartments. Again, the *japonica* and *O. glaberrima* cultivars clustered separately, whereas the *indica* cultivars were split between the *japonica* and *O. glaberrima* clusters. This clustering pattern is maintained in the rhizoplane communities (*SI Appendix*, Fig. S11 C and F); however, it breaks down in the endosphere compartment communities, which coincidentally are the least affected by rice genotype (12.8%,  $P = 0.005$ , WUF, *SI Appendix*, Fig. S11D and 8.5%,  $P = 0.028$ , UUF, *SI Appendix*, Fig. S11G).  $\alpha$ -Diversity measurements within the rhizosphere show a notable difference between the cultivars ( $P = 3.12E-06$ , ANOVA), with the *O. glaberrima* cultivars exhibiting high diversity relative to the *japonica* cultivars, especially in Arbuckle soil (Fig. 3B and Dataset S11). Again, the two *japonica* cultivars were more similar to the *indica* cultivar IR50, and the two *O. glaberrima* cultivars were more similar to the *indica* cultivar 93-11. These patterns in  $\alpha$ -diversity were not evident when examining other compartments (*SI Appendix*, Fig. S12). To explain which OTUs accounted for the genotypic effects in each rhizocompartment, we performed differential OTU abundance analyses between the cultivars (Dataset S12). In total, we found 125 OTUs that were affected by the plant genotype in at least one rhizocompartment. The rhizosphere had the most OTUs that were significantly impacted by genotype (*SI Appendix*, Fig. S13). This is consistent with the results from PERMANOVA and the CAP analyses.

**Geographical Effects on the Microbiomes of Field-Grown Plants.** We sought to determine whether the results from greenhouse plants were generalizable to cultivated rice and to investigate other factors that might affect the microbiome under field conditions. We therefore characterized the root-associated microbiomes of field rice plants distributed across eight geographically separate sites across California's Sacramento Valley (Fig. 4A). These eight sites were operated under two cultivation practices: organic cultivation and a more conventional cultivation practice termed “ecofarming” (see below). Because genotype explained the least variance in the greenhouse data, we limited the analysis to one cultivar, S102, a California temperate *japonica* variety that is widely cultivated by commercial growers and is closely related to M104 (26). Field samples were collected from vegetatively growing rice plants in flooded fields and the previously defined rhizocompartments were analyzed as before. Unfortunately, collection of bulk soil controls for the field experiment was not

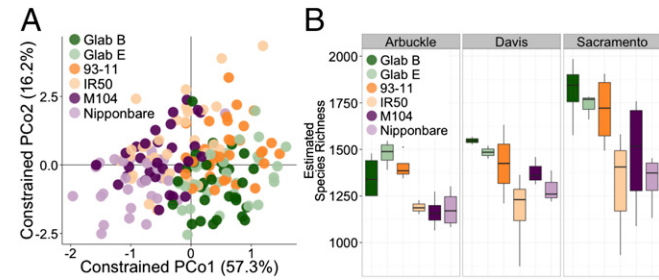


**Fig. 3.** Host plant genotype significantly affects microbial communities in the rhizospheric compartments. (A) Ordination of CAP analysis using the WUF metric constrained to rice genotype. (B) Within-sample diversity measurements of rhizosphere samples of each cultivar grown in each soil. Estimated species richness was calculated as  $e^{Shannon\_entropy}$ . The horizontal bars within boxes represent median. The tops and bottoms of boxes represent 75th and 25th quartiles, respectively. The upper and lower whiskers extend 1.5 $\times$  the interquartile range from the upper edge and lower edge of the box, respectively. All outliers are plotted as individual points.

possible, because planting densities in California commercial rice fields are too high to find representative soil that is unlikely to be affected by nearby plants. Amplification and sequencing of the field microbiome samples yielded 13,349,538 high-quality sequences (median: 54,069 reads per sample; range: 12,535–148,233 reads per sample; [Dataset S13](#)). The sequences were clustered into OTUs using the same criteria as the greenhouse experiment, yielding 222,691 microbial OTUs and 47,983 OTUs with counts >5 across the field dataset.

We found that the microbial diversity of field rice plants is significantly influenced by the field site.  $\alpha$ -Diversity measurements of the field rhizospheres indicated that the cultivation site significantly impacts microbial diversity ([SI Appendix, Fig. S14A](#),  $P = 2.00E-16$ , ANOVA and [Dataset S14](#)). Unconstrained PCoA using both the WUF and UUF metrics showed that microbial communities separated by field site across the first axis (Fig. 4B, WUF and [SI Appendix, Fig. S14B](#), UUF). PERMANOVA agreed with the unconstrained PCoA in that field site explained the largest proportion of variance between the microbial communities for field plants (30.4% of variance,  $P < 0.001$ , WUF, [Dataset S5O](#) and 26.6% of variance,  $P < 0.001$ , UUF, [Dataset S5P](#)). CAP analysis constrained to field site and controlled for rhizocompartment, cultivation practice, and technical factors (sequencing batch and biological replicate) agreed with the PERMANOVA results in that the field site explains the largest proportion of variance between the root-associated microbial communities in field plants (27.3%,  $P = 0.005$ , WUF, [SI Appendix, Fig. S15A](#) and 28.9%,  $P = 0.005$ , UUF, [SI Appendix, Fig. S15E](#)), suggesting that geographical factors may shape root-associated microbial communities.

**Rhizospheric Compartmentalization Is Retained in Field Plants.** Similar to the greenhouse plants, the rhizospheric microbiomes of field plants are distinguishable by compartment.  $\alpha$ -Diversity of the field plants again showed that the rhizosphere had the highest microbial diversity, whereas the endosphere had the least

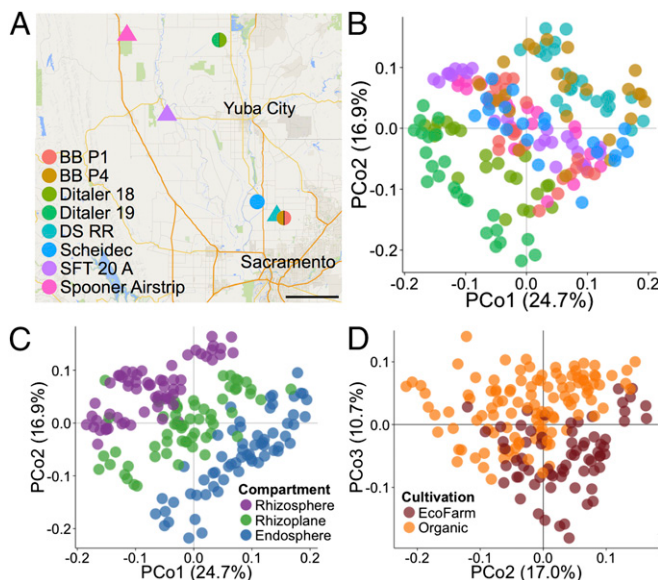


**Fig. 4.** Root-associated microbiomes from field-grown plants are separable by cultivation site, rhizospheric compartment, and cultivation practice. (A) Map depicting the locations of the field experiment collection sites across California's Central Valley. Circles represent organic-cultivated sites whereas triangles represent ecofarm-cultivated sites. (Scale bar, 10 mi.) (B) PCoA using the WUF method colored to depict the various sample collection sites. (C) Same PCoA in B colored by rhizospheric compartment. (D) Same PCoA in B and C depicting second and third axes and colored by cultivation practice.

diversity for all fields tested ([SI Appendix, Fig. S14A](#) and [Dataset S15](#)). PCoA of the microbial communities from field plants using the WUF and UUF distance metrics showed that the rhizocompartments separate across PCo 2 (Fig. 4C, WUF and [SI Appendix, Fig. S14C](#), UUF). PERMANOVA indicated that the separation in the rhizospheric compartments explained the second largest source of variation of the factors that were tested (20.76%,  $P < 0.001$ , WUF, [Dataset S5O](#) and 7.30%,  $P < 0.001$ , UUF, [Dataset S5P](#)). CAP analysis of the field plants' microbiomes constrained to the rhizocompartment factor and controlled for field site, cultivation practice, and technical factors agreed with PERMANOVA that a significant proportion of the variance between microbial communities is explained by rhizocompartment (20.9%,  $P = 0.005$ , WUF, [SI Appendix, Fig. S15C](#) and 10.9%,  $P = 0.005$ , UUF, [SI Appendix, Fig. S15G](#)).

Taxonomic distributions of phyla for the field plants were overall similar to the greenhouse plants: Proteobacteria, Chloroflexi, and Acidobacteria make up the majority of the rice microbiota. The taxonomic gradients from the rhizosphere to the endosphere are maintained in the field plants for Acidobacteria, Proteobacteria, Spirochaetes, Gemmatimonadetes, Armatimonadetes, and Planctomycetes. However, unlike for greenhouse plants, the distribution of Actinobacteria generally showed an increasing trend from the rhizosphere to the endosphere of field plants ([SI Appendix, Fig. S14E](#) and [Dataset S16](#)).

We again performed differential abundance tests between the OTUs in the compartments of field-grown plants ([SI Appendix, Fig. S16](#)). We found a set of 32 OTUs that were enriched in the endosphere compartment between every cultivation site, potentially representing a core field rice endospheric microbiome ([SI Appendix, Fig. S17](#)). The set of 32 OTUs consisted of Deltaproteobacteria in the genus *Anaeromyxobacter* and *Spirochaetes*, *Actinobacteria*, and *Alphaproteobacteria* in the family *Methylocystaceae*. Interestingly, 11 of the 32 core field endosphere OTUs were also found to be enriched in the endosphere compartment of greenhouse plants ([SI Appendix, Fig. S18](#)). Three of these OTUs were classifiable at the family level. These OTUs consisted of taxa in the families *Kineosporiaceae*, *Rhodocyclaceae*, and *Myxococcaceae*, all of which are also enriched in the *Arabidopsis* root endosphere microbiome (10).

**Cultivation Practice Results in Discernible Differences in the Microbiomes.** The rice fields that we sampled from were cultivated under two practices, organic farming and a variation of conventional cultivation called ecofarming (27). Ecofarming differs from organic farming in that chemical fertilizers, fungicide use, and herbicide use are all permitted but growth of transgenic rice and use of post-harvest fumigants are not permitted. Although cultivation practice itself does significantly affect  $\alpha$ -diversity of the rhizospheric compartments overall ( $P = 0.008$ , ANOVA; [Dataset S14](#)), there is also a significant interaction between the cultivation practice used and the rhizocompartments ( $P = 3.52E-07$ , ANOVA; [Dataset S14](#)), indicating that the  $\alpha$ -diversities of some rhizocompartments are affected differentially by cultivation practice. The  $\alpha$ -diversity within the rhizosphere compartment varied significantly by cultivation practice, with the mean  $\alpha$ -diversity being higher in ecofarmed rhizospheres than organic rhizospheres ( $P = 0.001$ , Wilcoxon test; [Dataset S14](#)), whereas not in the endosphere and rhizoplane microbial communities ( $P = 0.51$  and  $0.75$ , respectively, Wilcoxon tests; [Dataset S14](#)). Under nonconstrained PCoA, the cultivation practices are separable across principal coordinates 2 and 3 for both the WUF metric (Fig. 4D) and UUF metric ([SI Appendix, Fig. S14D](#)). PERMANOVA of the microbial communities was in agreement with the PCoAs in that cultivation practice has a significant impact on the rhizospheric microbial communities of field rice plants (8.47%,  $P < 0.001$ , WUF, [Dataset S5O](#) and 6.52%,  $P < 0.001$ , UUF, [Dataset S5P](#)). CAP analysis of the field plants constrained to cultivation practice agreed with the PERMANOVA results that there are significant differences between microbial communities from organic and ecofarmed rice plants (6.9% of the variance,

*P* = 0.005, WUF, *SI Appendix*, Fig. S15*D* and 7.0% of the variance, UUF, *P* = 0.005, *SI Appendix*, Fig. S15*H*).

To better understand which taxa account for the separation between organic and ecofarmed cultivated plants, we used a generalized linear model with a negative binomial distribution to identify OTUs that had significantly different abundance between the two cultivation practices in each rhizocompartment (*SI Appendix*, Fig. S19 and Dataset S18). Notably, organic cultivation farms were enriched for Alphaproteobacteria, Actinobacteria, and Gemmatimonadetes whereas ecofarmed samples were enriched in Deltaproteobacteria, Chloroflexi, and Spirochaetes (*SI Appendix*, Fig. S20). We examined OTUs from genera that have potential implications in promoting plant growth and appear to depend upon cultivation practice. OTUs belonging to known nitrogen-fixing genera were enriched in organically cultivated samples including the cyanobacterium *Anabaena* and the Alphaproteobacterial genera *Azospirillum* and *Rhodobacter* (*SI Appendix*, Fig. S21*A*). Organically cultivated samples were also enriched for Actinobacterial OTUs belonging to the genus *Streptomyces* (*SI Appendix*, Fig. S21*B* and *C*). Species within *Streptomyces* are known for their wide diversity of secondary metabolite production, many of which include antibiotic compounds (28). Microbial communities from ecofarmed rhizocompartments were enriched for OTUs that play a part in methane cycling belonging to the families *Syntrophorhabdaceae* (*SI Appendix*, Fig. S21*D* and *E*) and *Syntrophaceae*. Members from both of these families are known for syntrophic growth with methanogenic archaea (see below), providing these archaea with H<sub>2</sub> and formate essential for methane production (29–31).

**Microbes Involved in Methane Emissions.** Global rice cultivation accounts for a significant proportion of annual greenhouse gas emissions, primarily methane (32). Methane (CH<sub>4</sub>) emitted from rice paddies is mostly synthesized by methanogenic archaea. Although the majority of the CH<sub>4</sub> produced in rice paddy soil is oxidized by CH<sub>4</sub>-using eubacteria (33), much of the remaining CH<sub>4</sub> diffuses through the soil into the plant roots and is expelled via the aerenchyma tissue of the rice plant itself (19). We found a large difference in abundance of methanogenic archaea between the field plants and the greenhouse plants. Methanogenic archaea were in much higher abundance in the field plants than in the greenhouse plants, indicating that either the greenhouse conditions are not a suitable growth habitat for methanogenic archaea or that the soils used for the greenhouse study had a low initial abundance of methanogens (*SI Appendix*, Fig. S22*A–D*).

Methanogenic archaea require anaerobic conditions to function, and thus we did not expect methanogens to inhabit the endosphere or the rhizoplane. Surprisingly, the field plants exhibited high relative abundances of OTUs assigned to the genus *Methanobacterium* in the endosphere and rhizoplane that were comparable to or greater than the relative abundance of *Methanobacterium* in the rhizosphere (*SI Appendix*, Fig. S22*A*). This result is unexpected, given that the interior of rice roots is expected to have the highest levels of O<sub>2</sub> relative to other spatial compartments when grown in flooded soil. This pattern is not maintained with OTUs in other methanogenic genera including *Methanosarcina*, *Methanocella*, and *Methanosaeta*, however (*SI Appendix*, Fig. S22*B–D*). Relative abundance of these genera in field plants was always highest in the rhizosphere, where the O<sub>2</sub> concentration is expected to be relatively lower. To further confirm the presence of methanogenic archaea in the endosphere, we used an alternative approach by PCR amplification of the methyl coenzyme-M reductase (*mcrA*) gene, a gene essential for CH<sub>4</sub> production (34), from endosphere samples. By cloning and sequencing the *mcrA* amplicons, we again found that sequences derived from *Methanobacteriaceae* were in higher relative abundance in the endosphere than in the rhizosphere of field plants, whereas *Methanosarcina* sequences exhibited the opposite distribution (Dataset S19).

The relatively oxygenated environment within the rice roots might be expected to be suitable for CH<sub>4</sub> oxidation by methanotrophs. We found that in general the methanotrophic bacteria followed the expected trend of distribution across the rhizocompartments, with the relative abundance lowest in the rhizosphere and highest in the endosphere (*SI Appendix*, Fig. S22*E* and *F*). The field plants had higher abundances of methanotrophic bacteria compared with greenhouse plants, consistent with the low levels of methanogenic archaea and presumptive low levels of CH<sub>4</sub> production under greenhouse growth.

**Identification of Coabundance Networks of OTUs.** The sequence-based characterization of plant-associated microbiomes has primarily focused on how individual taxa within the microbiome associate with the host plant; however, the complex interactions that occur between taxa in the context of microbial communities are not revealed through this approach. Identification of microbial consortia is important for understanding their biological impact on the plant, but has been hindered by the inability to culture the vast majority of the microbes. It is likely that an important reason for the inability to grow many microbial species in pure culture can be attributed to consortium dynamics (35). Microbes cooperate in networks, supplying each other with critical nutrients for growth and survival. For example, methanogenic archaea cooperate with syntrophic partners to obtain H<sub>2</sub> and formate for CH<sub>4</sub> synthesis; hydrogen consumption by the methanogen allows the secondary fermentation process by the syntroph to become energetically favorable (29, 35).

We hypothesized that it might be possible to identify consortia that are involved in CH<sub>4</sub> cycling by generating OTU coabundance modules from the list of differentially abundant OTUs from the field experiment. We used an approach similar to gene coexpression network construction to generate the OTU coabundance modules. Briefly, pairwise Pearson correlations between OTUs determined to be differentially abundant between experimental factors included in the field experiment (10,848 OTUs; Datasets S16 and S17) were calculated and used as a distance metric for hierarchical clustering into a dendrogram, which was then dynamically pruned to form 284 coabundance modules (Dataset S20). The resulting modules were queried for clusters containing taxa that belonged to methanogenic archaea including *Methanobacterium*, *Methanosarcina*, *Methanocella*, and *Methanosaeta*. We identified 15 modules containing methanogenic OTUs with a correlation of 0.6 or greater to other OTUs within the same module (11 shown in Fig. 5*A*; Dataset S21). Modules containing methanogenic taxa were enriched for OTUs with methanotrophic, syntrophic, and CH<sub>4</sub> cycling potential (hypergeometric test, Dataset S22; Fig. 5*B* and *SI Appendix*, Fig. S23). Many of the remaining OTUs in the methanogenic modules have limited taxonomic information or functional information available, thus making functional inference difficult. Taken together, these results show that an OTU coabundance network approach is successful in generating associations that can recapitulate empirical data, and therefore might have predictive value for identifying novel microbial associations.

**Acquisition of Microbiomes by the Root.** We have shown that rice seedlings grown in field soil in the greenhouse acquire microbiomes that exhibit characteristics similar to those of field rice plants, in terms of the general distribution of phyla in the rhizocompartments. To understand the dynamics of microbiome acquisition from soil, we performed a time-series experiment. We transplanted steriley germinated seedlings of the *japonica* M104 cultivar into soil collected from the rice field in Davis in the greenhouse and collected samples at increasing intervals (0, 1, 2, 3, 5, 8, and 13 d). To monitor general changes in the soil microbial communities, we sampled from pots containing unplanted soil in the same container at each time point.

After collection, 16S rRNA gene sequencing of the samples from different compartments was performed as before. We used the proportion of microbial reads to organellar (plastidial

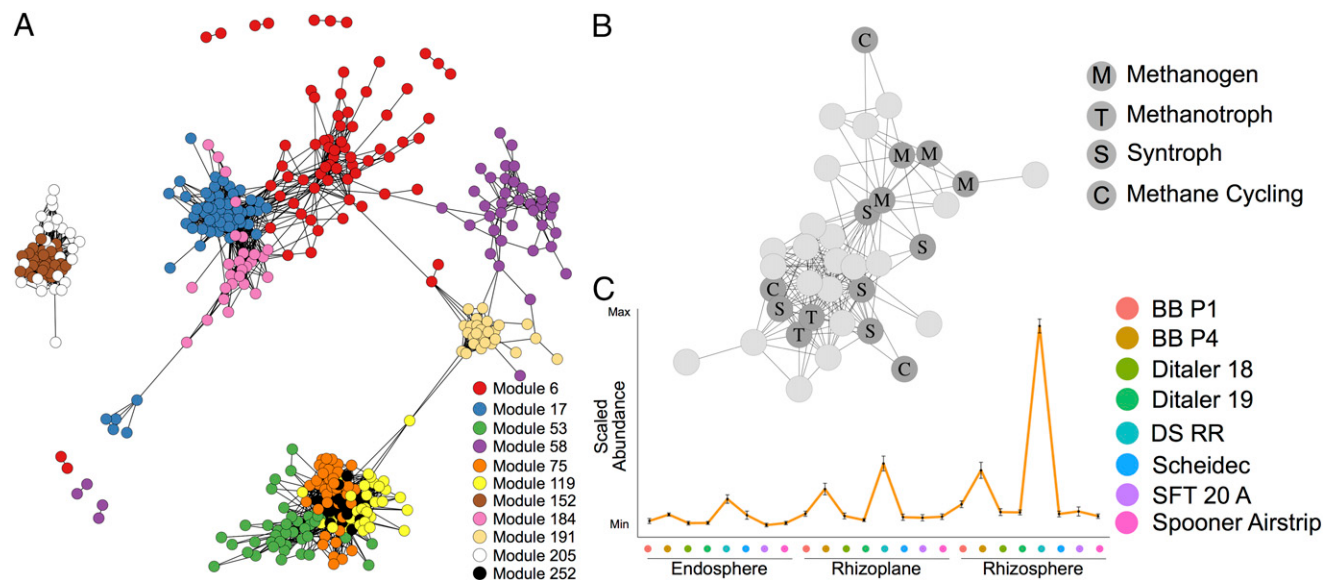


**Fig. 5.** OTU coabundance network reveals modules of OTUs associated with methane cycling. (A) Subset of the entire network corresponding to 11 modules with methane cycling potential. Each node represents one OTU and an edge is drawn between OTUs if they share a Pearson correlation of greater than or equal to 0.6. (B) Depiction of module 119 showing the relationship between methanogens, syntrophs, methanotrophs, and other methane cycling taxonomies. Each node represents one OTU and is labeled by the presumed function of that OTU's taxonomy in methane cycling. An edge is drawn between two OTUs if they have a Pearson correlation of greater than or equal to 0.6. (C) Mean abundance profile for OTUs in module 119 across all rhizocompartments and field sites. The position along the x axis corresponds to a different field site. Error bars represent SE. The x and y axes represent no particular scale.

and mitochondrial) reads to analyze microbial abundance in the endosphere over time (Fig. 6*A*). Using this technique, we confirmed the sterility of seedling roots before transplantation. We found that microbial penetration into the endosphere occurred at or before 24 h after transplantation and that the proportion of microbial reads to organellar reads increased over the first 2 wk after transplantation (Fig. 6*A*). To further support the evidence for microbiome acquisition within the first 24 h, we sampled root endospheric microbiomes from steriley germinated seedlings before transplanting into Davis field soil as well as immediately after transplantation and 24 h after transplantation (*SI Appendix*, Fig. S24). The root endospheres of steriley germinated seedlings, as well as seedlings transplanted into Davis field soil for 1 min, both had a very low percentage of microbial reads compared with organellar reads (0.22% and 0.71%), with the differences not statistically significant ( $P = 0.1$ , Wilcoxon test). As before, endospheric microbial abundance increased significantly, by >10-fold after 24 h in field soil (3.95%,  $P = 0.05$ , Wilcoxon test). We conclude that brief soil contact does not strongly increase the proportion of microbial reads, and therefore the increase in microbial reads at 24 h is indicative of endophyte acquisition within 1 d after transplantation.

$\alpha$ -Diversity significantly varied by rhizocompartment ( $P < 2E-16$ ; Dataset S23) and there was a significant interaction between rhizocompartment and collection time ( $P = 0.042$ ; Dataset S23); however, when each rhizocompartment was analyzed individually, the bulk soil was the only compartment that showed a significant amount of variation in  $\alpha$ -diversity over time (*SI Appendix*, Fig. S25 and Dataset S23). The above results suggest that a diverse microbiota can begin to colonize the rhizoplane and endosphere as early as 24 h after transplanting into soil. We next evaluated how  $\beta$ -diversities shift over time in each rhizocompartment. We compared the time-series microbial communities with the previous greenhouse experiment microbial communities of M104 in Davis soil (Fig. 6*B* and *C*).  $\beta$ -Diversity measurements of the time-series data indicated that microbiome samples from each compartment are separable by time. Furthermore, the rhizoplane and endosphere microbiomes from the later time point in the time-series data

(13 d) approach the endosphere and rhizoplane microbiome compositions for plants that have been grown in the greenhouse for 42 d.

There are slight shifts in the distribution of phyla over time; however, there are significant distinctions between the compartments starting as early as 24 h after transplantation into soil (Fig. 6*D*, *SI Appendix*, Figs. S24B and S26, and Dataset S24). Because each phylum consists of diverse OTUs that could exhibit very different behaviors during acquisition, we next examined the dynamics and colonization patterns of specific OTUs within the time-course experiment. The core set of 92 endosphere-enriched OTUs obtained from the previous greenhouse experiment (*SI Appendix*, Fig. S9C) was analyzed for relative abundances at different time points (Fig. 6*E*). Of the 92 core endosphere-enriched microbes present in the greenhouse experiment, 53 OTUs were detectable in the endosphere in the time-course experiment. The average abundance profile over time revealed a colonization pattern for the core endospheric microbiome. Relative abundance of the core endosphere-enriched microbiome peaks early (3 d) in the rhizosphere and then decreases back to a steady, low level for the remainder of the time points. Similarly, the rhizoplane profile shows an increase after 3 d with a peak at 8 d with a decline at 13 d. The endosphere generally follows the rhizoplane profile, except that relative abundance is still increasing at 13 d. These results suggest that the core endospheric microbes are first attracted to the rhizosphere and then locate to the rhizoplane, where they attach before migration to the root interior. To summarize, microbiome acquisition from soil appears to occur relatively rapidly, initiating within 24 h and approaching steady state within 14 d. The dynamics of accumulation suggest a multistep process, in which the rhizosphere and rhizoplane are likely to play key roles in determining the compositions of the interior and exterior components of the root-associated microbiome (*Discussion*).

## Discussion

**Factors Affecting the Composition of Root-Associated Microbiomes.** The data presented here provide a characterization of the microbiome of rice, involving the combination of finer structural

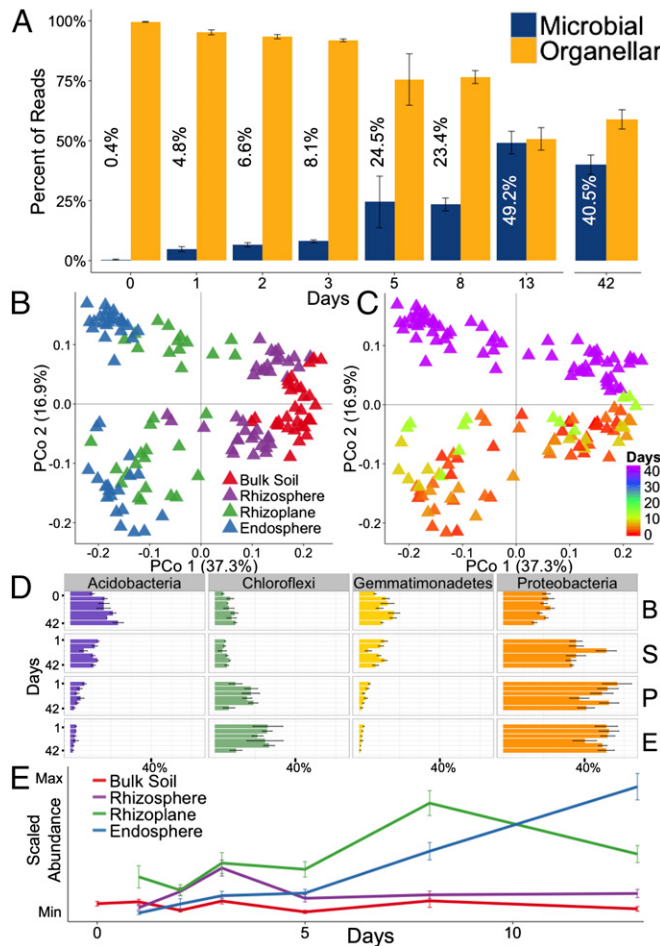


**Fig. 6.** Time-series analysis of root-associated microbial communities reveals distinct microbiome colonization patterns. (A) Ratios of microbial to organellar (plastidial and mitochondrial) 16S rRNA gene reads in the endosphere after transplantation into Davis soil. The 42-d time point corresponds to the earlier greenhouse experiment data (Fig. 1) subsetted to M104 in Davis soil. Mean percentages of the ratios are depicted with each bar. (B) PCoA of the time-series experiment and the greenhouse experiment subsetted to plants growing in Davis soil and colored by rhizospheric compartment. (C) The same PCoA as in B colored by collection day after transplantation into soil. (D) Average relative abundance for select phyla over the course of microbiome acquisition. (E) Average abundance profile of 53 out of the 92 core endosphere-enriched OTUs in each rhizospheric compartment. Error bars represent SE.

resolution and deeper sequencing than previous plant microbiome studies and using both controlled greenhouse and field studies covering a geographical range of cultivation. Specifically, we have been able to characterize in-depth the compositions of three distinct rhizocompartments—the rhizosphere, rhizoplane, and endosphere—and gain insights into the effects of external factors on each of these compartments. We note that a detailed characterization of plant rhizoplane microbiota in relation to the rhizosphere and the endosphere has not been previously attempted. To achieve this, we successfully adapted protocols for removal of rhizoplane microbes from the endosphere of *Arabidopsis* roots (9, 10). Because the fractional abundance of organellar reads in the rhizosphere, rhizoplane, and endosphere exhibits a clear increasing gradient (*SI Appendix*, Fig. S27), we hypothesize that we are isolating the rhizoplane fraction via disruption of the rhizodermis, consistent with direct EM observations on *Arabidopsis* roots following sonication (9, 10). The fine structure approach we have used combined with depth of sequencing allowed us to analyze over 250,000 OTUs, an order

of magnitude greater than in any single plant species to date. Under controlled greenhouse conditions, the rhizocompartments described the largest source of variation in the microbial communities sampled (*Dataset S5A*). The pattern of separation between the microbial communities in each compartment is consistent with a spatial gradient from the bulk soil across the rhizosphere and rhizoplane into the endosphere (Fig. 1C). Similarly, microbial diversity patterns within samples hold the same pattern where there is a gradient in  $\alpha$ -diversity from the rhizosphere to the endosphere (Fig. 1B). Enrichment and depletion of certain microbes across the rhizocompartments indicates that microbial colonization of rice roots is not a passive process and that plants have the ability to select for certain microbial consortia or that some microbes are better at filling the root colonizing niche. Similar to studies in *Arabidopsis*, we found that the relative abundance of Proteobacteria is increased in the endosphere compared with soil, and that the relative abundances of Acidobacteria and Gemmatimonadetes decrease from the soil to the endosphere (9–11), suggesting that the distribution of different bacterial phyla inside the roots might be similar for all land plants (Fig. 1D and *Dataset S6*). Under controlled greenhouse conditions, soil type described the second largest source of variation within the microbial communities of each sample. However, the soil source did not affect the pattern of separation between the rhizospheric compartments, suggesting that the rhizocompartments exert a recruitment effect on microbial consortia independent of the microbiome source.

By using differential OTU abundance analysis in the compartments, we observed that the rhizosphere serves an enrichment role for a subset of microbial OTUs relative to bulk soil (Fig. 2). Further, the majority of the OTUs enriched in the rhizosphere are simultaneously enriched in the rhizoplane and/or endosphere of rice roots (Fig. 2B and *SI Appendix*, Fig. S16B), consistent with a recruitment model in which factors produced by the root attract taxa that can colonize the endosphere. We found that the rhizoplane, although enriched for OTUs that are also enriched in the endosphere, is also uniquely enriched for a subset of OTUs, suggesting that the rhizoplane serves as a specialized niche for some taxa. Conversely, the vast majority of microbes depleted in the rhizoplane are also depleted in the endosphere (Fig. 2C and *SI Appendix*, Fig. S16C), suggesting that the selectivity for colonization of the interior occurs at the rhizoplane and that the rhizoplane may serve an important gating role for limiting microbial penetration into the endosphere. It is important to note that the community structure we observe in each compartment is likely not simply caused by the plant alone. Microbial community structural differences between the compartments may be attributable also to microbial interactions involving both competition and cooperation.

In the case of field plants, we observed that the largest source of microbiome separation was due to cultivation site, rather than the spatial compartments (*Dataset S5 O* and *P*). These results are in contrast to the controlled greenhouse experiment where the soil effect was the second largest source of variation, suggesting the geography may be more important for determining the composition of the root microbiome than soil structure alone (*Dataset S5A*). These results differ from the results in the maize microbiome study, where microbial communities showed clear separation by state but not very much by geographic location within the same state (12). However, we note that in our study the locations within California were separated by distances of up to ~125 km, vs. a maximum separation of ~40 km in the intrastate locations of the maize study. Other factors that might account for the different results in our study include the number of field sites examined (eight, vs. three intrastate fields examined in the maize study), increased sequencing depth, different resolution because spatial compartments in maize roots were not separately analyzed, or possibly intrinsic differences between cultivated rice and maize.

Our design of the field experiment allowed us to test for cultivation practice effects on the rice root-associated microbiome,

specifically between organic cultivation and ecofarming, a more conventional cultivation practice. We found that cultivation practice described a significant amount of variation between the microbiomes, and that this effect was exhibited across every rhizospheric compartment (Fig. 4D and *SI Appendix*, Fig. S14D). These results are in contrast to the maize microbiome study, where an organically cultivated field had no significant separation from a conventionally cultivated field in the same state (12). Again, the difference in results between the two studies might be due to differences in sequencing depth and structural resolution or to intrinsic differences between the crops.

#### **Microbial Consortia Associated with Methane Cycling in Rice Fields.**

Rice cultivation is a large contributor to agricultural CH<sub>4</sub> emissions due to the anaerobic conditions resulting from flooded fields. Currently, the model for CH<sub>4</sub> emissions under rice cultivation is that CH<sub>4</sub> is formed in the soil away from the roots and diffuses through the soil to the rice root, where it is expelled via the aerenchyma in the roots (19, 32, 36). We used our dataset to examine the abundances of taxa related to CH<sub>4</sub> cycling. As predicted, we observed that the relative abundance of some methanogens (*Methanocella*, *Methanosarcina*, and *Methanosaeta*) is higher in the rhizosphere than in the endosphere (*SI Appendix*, Fig. S22). However, the relative abundance of the methanogen *Methanobacterium* was found to be typically equal or higher in the endosphere than in the rhizosphere. This is an unexpected finding, because the root interior is relatively O<sub>2</sub>-rich and therefore unfavorable for anaerobic archaea. How these archaea might survive within the root and whether they are contributing to CH<sub>4</sub> production at this interior location are questions that should be investigated. These results indicate that our understanding of rice-associated CH<sub>4</sub> production is still incomplete, and emphasize the need for more detailed studies to elucidate the different players and their roles in the process, perhaps using metagenomic and metatranscriptomic sequencing to better understand the metabolic potential of endosphere microbial communities.

An approach toward unraveling methanogen interactions with rice roots that we have explored is the construction of OTU coabundance networks. We hypothesized that microbes producing or using CH<sub>4</sub> might form consortia that would be revealed through this analysis. The sequencing depth and variation provided by the field experiment allowed us to test this approach by generating clusters of OTUs and identification of clusters containing methanogenic archaea. Inspection of individual OTUs within such clusters revealed additional taxonomies known to be involved in CH<sub>4</sub> cycling, such as methanotrophic, syntrophic, and CH<sub>4</sub>-cycling eubacteria (Fig. 5 and *SI Appendix*, Fig. S23). The clusters also contained OTUs with no known role in CH<sub>4</sub> cycling. Possibly these OTUs represent novel players that have been revealed through this approach, although larger-scale studies with additional field sites will be needed to validate the significance of their associations. Even with this limited scale, the results of this analysis are very encouraging. This approach might be generalizable for culture-independent identification of other microbial consortia involved in different types of geochemical cycles that interact with plant roots. However, this approach might be more applicable to those microbial lineages that are tightly linked to certain traits, such as CH<sub>4</sub> cycling, and might not be successful when a trait is much more widespread independent of lineage, such as nitrogen fixation.

**A Multistep Model for Microbiome Acquisition.** Studies on mammals have established that the fetus at birth already has a microbiome derived from the mother, and that diet and other environmental factors further shape the gut microbiome (37–39). For plants, the process of microbiome acquisition is not well-understood (7). Microbiome transmission through the embryo seems unlikely, because surface sterilization of the seeds resulted in axenic plants (Fig. 6A and *SI Appendix*, Fig. S23). Our success in obtaining in-depth sequence coverage for all three different spatial compartments in the root provided us with an opportunity to address

this question by carrying out a time-staged profiling of the microbial compositions of the compartments during the early stages of microbiome acquisition. We find that microbiome acquisition from soil is rapid, namely that rice plants begin to assemble an endospheric microbiome within a day after transplantation from sterile media to soil, and the relative level approaches steady state within 2 wk. The 13-d endosphere and rhizoplane microbiomes were most similar to the older, 42-d, microbiomes from the previous greenhouse experiment that we consider to represent steady state, as the latter microbiomes are from well-established vegetatively growing plants (Fig. 6B and C). Because separate batches of soil were used between the greenhouse and the acquisition experiment, it is important to note that the microbiomes may not be directly comparable across different experiments, due to seasonal variation between soil batches (9–11). The patterns of relative abundance in phyla between the compartments (e.g., higher proportions of Acidobacteria in the rhizosphere than endosphere and lower proportions of Proteobacteria and Chloroflexi in the rhizosphere than endosphere) are evident within 24 h after the rice plants were transplanted into soil (Fig. 6C and *SI Appendix*, Figs. S24B and S26). Based on studies of the steady-state microbiomes of the rhizosphere and endosphere, it has been proposed that plants might assemble their microbiomes in two steps, with the first step involving a general recruitment to the vicinity of the root and a second step for entry inside the root that involves species-specific genetic factors (7). The dynamics of microbiome acquisition in our study provide experimental support for this model, in that the general concept of recruitment and assembly as separate steps is consistent with our data. We observed an initial enrichment in the rhizosphere, consistent with the attraction of a diverse set of microbes to the vicinity of the plant, followed by slower rates of accumulation of OTUs in the endosphere (Fig. 6E). The selectivity of the latter process is also implied by the extensive depletion of rhizospheric OTUs in the endosphere. However, when rhizoplane microbiome data are taken into consideration, microbiome acquisition in the root appears to be a more complex multistep process, in which the rhizoplane plays a key role. After initial recruitment to the rhizosphere, only a subset of these microbes initially recruited to the rhizosphere are bound to the root surface at the rhizoplane, suggesting selectivity for direct physical association with the root. This selection may occur by the plant, or may occur through the ability to form biofilms, as certain microbes are known to form biofilms along root surfaces (40, 41). A further selective step must operate to account for the additional depletion of rhizoplane OTUs from the endosphere at steady state, implying that binding is not sufficient for entry. Binding at the rhizoplane might, however, act as a necessary prerequisite for endospheric OTUs, as the time course shows that accumulation of OTUs at the rhizoplane precedes that in the endosphere. We suggest that the rhizoplane serves a critical gating role; of the microbes that are attracted to the rhizosphere, only a subset can bind the rhizoplane, and a fraction of these are permitted to enter and proliferate in the endosphere. Each of these steps likely involves molecular signals from the plant, presumptively components of root exudates and possibly cell-wall components or membrane proteins. The signals could consist of general plant metabolites as well as species- and genotype-specific molecules. In the model proposed by Bulgarelli et al. (7), genotype signals are proposed to regulate entry into the endosphere. However, in our study, the rhizosphere composition showed the largest variation in the comparison of different cultivars, suggesting that the genotypic factors appear to also act at the level of general microbial recruitment. In summary, the dynamic shifts in microbiomes across each compartment indicate that the actions of three or more selective steps at distinct spatial locations from the root interior, and responding to multiple signals from the plant, coordinate the assembly of the root microbiome.

## Materials and Methods

Microbial communities from the rhizosphere, rhizoplane, and root endosphere of various rice cultivars grown in the greenhouse and field were profiled by amplifying fragments of the 16S rRNA gene and sequenced using the Illumina MiSeq platform. The sequence analysis was carried out using the QIIME pipeline (42) and all statistical analyses were performed using R v3.1.0 (43). Further details of materials and methodology are explained in *SI Appendix, Materials and Methods*. The raw sequencing reads for this project were submitted to the National Center for Biotechnology Information Short Read Archive under accession no. SRP044745. The custom scripts used for analyzing the data presented here can be found at [github.com/ricemicrobiome/edwards-et-al.-2014](http://github.com/ricemicrobiome/edwards-et-al.-2014).

1. Tringe SG, et al. (2005) Comparative metagenomics of microbial communities. *Science* 308(5721):554–557.
2. Zhang H, et al. (2009) A soil bacterium regulates plant acquisition of iron via deficiency-inducible mechanisms. *Plant J* 58(4):568–577.
3. Long SR (1989) Rhizobium-legume nodulation: Life together in the underground. *Cell* 56(2):203–214.
4. Bolan N (1991) A critical review on the role of mycorrhizal fungi in the uptake of phosphorus by plants. *Plant Soil* 134(2):189–207.
5. Bais HP, Weir TL, Perry LG, Gilroy S, Vivanco JM (2006) The role of root exudates in rhizosphere interactions with plants and other organisms. *Annu Rev Plant Biol* 57: 233–266.
6. Berendsen RL, Pieterse CM, Bakker PA (2012) The rhizosphere microbiome and plant health. *Trends Plant Sci* 17(8):478–486.
7. Bulgarelli D, Schlaepff K, Spaepen S, Ver Loren van Themaat E, Schulze-Lefert P (2013) Structure and functions of the bacterial microbiota of plants. *Annu Rev Plant Biol* 64: 807–838.
8. Mendes R, et al. (2011) Deciphering the rhizosphere microbiome for disease-suppressive bacteria. *Science* 332(6033):1097–1100.
9. Bulgarelli D, et al. (2012) Revealing structure and assembly cues for *Arabidopsis* root-inhabiting bacterial microbiota. *Nature* 488(7409):91–95.
10. Lundberg DS, et al. (2012) Defining the core *Arabidopsis thaliana* root microbiome. *Nature* 488(7409):86–90.
11. Schlaepff K, Dombrowski N, Oter RG, Ver Loren van Themaat E, Schulze-Lefert P (2014) Quantitative divergence of the bacterial root microbiota in *Arabidopsis thaliana* relatives. *Proc Natl Acad Sci USA* 111(2):585–592.
12. Peiffer JA, et al. (2013) Diversity and heritability of the maize rhizosphere microbiome under field conditions. *Proc Natl Acad Sci USA* 110(16):6548–6553.
13. Gottle NR, et al. (2011) Distinct microbial communities within the endosphere and rhizosphere of *Populus deltoides* roots across contrasting soil types. *Appl Environ Microbiol* 77(17):5934–5944.
14. Shakya M, et al. (2013) A multifactor analysis of fungal and bacterial community structure in the root microbiome of mature *Populus deltoides* trees. *PLoS ONE* 8(10): e76382.
15. Palmer C, Bik EM, DiGiulio DB, Relman DA, Brown PO (2007) Development of the human infant intestinal microbiota. *PLoS Biol* 5(7):e177.
16. Dominguez-Bello MG, et al. (2010) Delivery mode shapes the acquisition and structure of the initial microbiota across multiple body habitats in newborns. *Proc Natl Acad Sci USA* 107(26):11971–11975.
17. Sessitsch A, et al. (2012) Functional characteristics of an endophyte community colonizing rice roots as revealed by metagenomic analysis. *Mol Plant Microbe Interact* 25(1):28–36.
18. Krief C, et al. (2012) Metaproteogenomic analysis of microbial communities in the phyllosphere and rhizosphere of rice. *ISME J* 6(7):1378–1390.
19. Neue H-U (1993) Methane emission from rice fields. *Bioscience* 43(7):466–474.
20. McMurdie PJ, Holmes S (2014) Waste not, want not: Why rarefying microbiome data is inadmissible. *PLOS Comput Biol* 10(4):e1003531.
21. Im W-T, Kim S-H, Kim MK, Ten LN, Lee S-T (2006) *Pleomorphomonas koreensis* sp. nov., a nitrogen-fixing species in the order *Rhizobiales*. *Int J Syst Evol Microbiol* 56(Pt 7):1663–1666.
22. Madhaiyan M, et al. (2013) *Pleomorphomonas diazotrophica* sp. nov., an endophytic N-fixing bacterium isolated from root tissue of *Jatropha curcas* L. *Int J Syst Evol Microbiol* 63(Pt 7):2477–2483.
23. Xie C-H, Yokota A (2005) *Pleomorphomonas oryzae* gen. nov., sp. nov., a nitrogen-fixing bacterium isolated from paddy soil of *Oryza sativa*. *Int J Syst Evol Microbiol* 55(Pt 3):1233–1237.
24. Ransom-Jones E, Jones DL, McCarthy AJ, McDonald JE (2012) The *Fibrobacteres*: An important phylum of cellulose-degrading bacteria. *Microb Ecol* 63(2):267–281.
25. Leschine SB (1995) Cellulose degradation in anaerobic environments. *Annu Rev Microbiol* 49:399–426.
26. Kim S-I, Tai TH (2013) Identification of SNPs in closely related *temperate japonica* rice cultivars using restriction enzyme-phased sequencing. *PLoS ONE* 8(3):e60176.
27. Lundberg Family Farm (2014) Organic vs. eco-farmed. Available at [www.lundberg.com/commitment/ecofarmed.aspx](http://www.lundberg.com/commitment/ecofarmed.aspx). Accessed July 14, 2014.
28. Watve MG, Tickoo R, Jog MM, Bhole BD (2001) How many antibiotics are produced by the genus *Streptomyces*? *Arch Microbiol* 176(5):386–390.
29. Stams AJ, Plugge CM (2009) Electron transfer in syntrophic communities of anaerobic bacteria and archaea. *Nat Rev Microbiol* 7(8):568–577.
30. Gray ND, et al. (2011) The quantitative significance of *Syntrophaceae* and syntrophic partnerships in methanogenic degradation of crude oil alkanes. *Environ Microbiol* 13(11):2957–2975.
31. Schink B (1997) Energetics of syntrophic cooperation in methanogenic degradation. *Microbiol Mol Biol Rev* 61(2):262–280.
32. Conrad R (2009) The global methane cycle: Recent advances in understanding the microbial processes involved. *Environ Microbiol Rep* 1(5):285–292.
33. Holzapfel-Pschorn A, Conrad R, Seiler W (1985) Production, oxidation and emission of methane in rice paddies. *FEMS Microbiol Lett* 31(6):343–351.
34. Thauer RK (1998) Biochemistry of methanogenesis: A tribute to Marjory Stephenson. *Microbiology* 144(Pt 9):2377–2406.
35. McInerney MJ, Sieber JR, Gunsalus RP (2009) Syntrophy in anaerobic global carbon cycles. *Curr Opin Biotechnol* 20(6):623–632.
36. Lee HJ, Kim SY, Kim PJ, Madsen EL, Jeon CO (2014) Methane emission and dynamics of methanotrophic and methanogenic communities in a flooded rice field ecosystem. *FEMS Microbiol Ecol* 88(1):195–212.
37. Gueimonde M, et al. (2006) Effect of maternal consumption of *Lactobacillus GG* on transfer and establishment of fecal bifidobacterial microbiota in neonates. *J Pediatr Gastroenterol Nutr* 42(2):166–170.
38. Vaishampayan PA, et al. (2010) Comparative metagenomics and population dynamics of the gut microbiota in mother and infant. *Genome Biol Evol* 2:53–66.
39. Koenig JE, et al. (2011) Succession of microbial consortia in the developing infant gut microbiome. *Proc Natl Acad Sci USA* 108(Suppl 1):4578–4585.
40. Bais HP, Fall R, Vivanco JM (2004) Biocontrol of *Bacillus subtilis* against infection of *Arabidopsis* roots by *Pseudomonas syringae* is facilitated by biofilm formation and surfactin production. *Plant Physiol* 134(1):307–319.
41. Walker TS, et al. (2004) *Pseudomonas aeruginosa*-plant root interactions. Pathogenicity, biofilm formation, and root exudation. *Plant Physiol* 134(1):320–331.
42. Caporaso JG, et al. (2010) QIIME allows analysis of high-throughput community sequencing data. *Nat Methods* 7(5):335–336.
43. R Core Team (2012) R: A Language and Environment for Statistical Computing (R Found Stat Comput, Vienna).

**ACKNOWLEDGMENTS.** We thank Lance Benson and Jessica Lundberg of Lundberg Family Farms; George Tibbets and Michael Lear for generously providing samples and access to their field facilities; Derek Lundberg and Jeffery Dangl (The University of North Carolina) for sharing their protocol for root sonication prior to publication; Kelsey Galimba, John Jaeger, Cassandra Ramos, and Paul Tisher for technical assistance at the early stages of the project; Gurdev Khush and Kate Scow for valuable advice; and members of the J.A.E. and V.S. laboratories for helpful discussions. J.A.E. and V.S. acknowledge the support of National Science Foundation Awards DBI-0923806 and IOS-1444974; J.E. acknowledges partial support from the Henry A. Jastro Graduate Research Award; and C.S.-M. acknowledges support from the University of California Institute for Mexico (UCMEXUS)/Consejo Nacional de Ciencia y Tecnología (CONACYT) and Secretaría de Educación Pública (Mexico).

1    **Supplementary Information**

2    Edwards et al. PNAS

3

4    **Soil collection for greenhouse experiment and microbiome acquisition experiment**

5              Soil from the rice field in Sacramento (38.58575 degrees north and -121.596911 West) was  
6    collected on 3/15/2013 using shovels to gather down to a depth of approximately 8 inches. Soil from the  
7    rice field in Arbuckle, CA (39.011732 degrees North and -121.92212 degrees West) was collected on  
8    3/18/2013 using a front-end loader to gather down to a depth of approximately 8 inches. Soil from a rice  
9    field in Davis, CA (38.543864 degrees North and -121.81223 West) was collected on 3/19/2013 using  
10   shovels to gather down to a depth of approximately 8 inches. All soils were transported back to the  
11   greenhouse and stored until planting on 3/28/2013. All soils were mixed individually in clean tubs to  
12   homogenize the soil. The soil was placed into new 5 x 5 inch pots that were then placed into tubs (24  
13   pots each). Each tub contained only one soil type in order to avoid microbial mixing between the soils.  
14   Each tub was watered in order to submerge the soils as suited to rice cultivation. Soil from the Davis field  
15   was collected for the microbiome acquisition experiment on 11/26/2013 using the same method as  
16   described above. Soil samples for the Arbuckle, Davis, and Sacramento fields were analyzed at the UC  
17   Davis Analytical Lab for chemical content (Dataset S8).

18    **Plant germination, transplantation, and cultivation in the greenhouse and microbiome acquisition  
19    experiment**

20              Seeds from 6 cultivated varieties (M104, Nipponebare, IR50, 93-11, TOg 7102, and TOg 7267)  
21    were dehulled, surface sterilized in 70% bleach for 5 minutes and steriley germinated on MS agar media  
22    in the dark. After germination, the rice seedlings were transplanted into the various soils in the  
23    greenhouse. The tubs were watered every other day and nutrients were supplied to each tub on 2-week  
24    basis on 4/12/2013 and 4/26/2013. All weeds were manually removed from the pots when identified.

25        For the microbiome acquisition experiment, M104 seeds were dehulled and surface sterilized in  
26      bleach for 5 minutes and subsequently germinated on MS agar media in the dark. The seedlings were  
27      transplanted into Davis soil in the greenhouse and sampled according to the time series using the same  
28      protocol for sample collection detailed above.

29      **Experimental design for greenhouse and microbiome acquisition experiments**

30        The greenhouse experiment was designed as a split-split plot experiment. Briefly, there were 12  
31      tubs total so that each soil had 4 tubs. We collected only one rhizocompartment from each pot such that  
32      each every rhizocompartment was taken from every cultivar once per tub, giving a total of 18  
33      rhizocompartment samples and 6 bulk soil samples per tub (Dataset S1). Because the selected cultivars  
34      flower at various times, to avoid confounding issues between developmental stages and cultivar effects  
35      we collected all samples at 42 days while all cultivars were still vegetatively growing.

36        The plants for the acquisition experiment were all contained in one large tub along with unplanted  
37      pots for bulk soil controls. Each plant collected had all three rhizocompartments sampled.

38      **Experimental design of the field experiment**

39        All fields sampled in the field experiment are managed by Lundberg Family Farms (Richvale,  
40      CA, USA). All of these fields are subject to typical California rice cultivation practices (presoaked seeds,  
41      aerial seeding, dense planting, etc), with the cultivation differences being between “eco farming” and  
42      organic farming of the fields. 8 individual plants were sampled per field site (Dataset S1).

43      **Sample Collection of Rhizosphere, Rhizoplane, and Endosphere Fractions**

44        Samples were collected over a 4-day period from 5/6/2013 to 5/9/2013. The soil and plant were  
45      removed from each pot and the roots were removed from the soil. We avoided collecting any roots that  
46      were at the interface of the pot and the soil in order to avoid false environments. The excess soil was  
47      manually shaken from the roots, leaving approximately 1mm of soil still attached to the roots (Fig. S2).  
48      We separated the 1mm of soil from the roots directly in the greenhouse by placing the roots with soil still  
49      attached in a sterile flask with 50 ml of sterile Phosphate Buffered Saline (PBS) solution. The roots were  
50      then stirred vigorously with sterile forceps in order to clean all the soil from the root surfaces. The soil

51 that was cleaned from the roots was poured into a 50ml Falcon tube and stored as the rhizosphere  
52 compartment at 4°C until DNA extraction the same day.

53       The roots designated for rhizoplane collection were cleaned in the greenhouse and placed in a  
54 Falcon tube with 15 ml PBS, and tightly adhering microbes at the root surface were removed using a  
55 sonication protocol originally developed for Arabidopsis roots (1-3). The roots in the Falcon tube were  
56 sonicated for 30 s at 50-60 Hz (output frequency 42 kHz, power 90 W, Branson Unltrasonics). The  
57 sonication procedure strips the rhizoplane microbes from the root surface as well as portions of the  
58 rhizodermis as evidenced by the gradient of organellar reads from the rhizoplane to the endosphere (Fig.  
59 S27). The roots were then removed and discarded and the liquid PBS fraction was kept as the rhizoplane  
60 compartment.

61       The roots designated for the endosphere collection were cleaned and sonicated as described  
62 before. Two more sonication procedures using clean PBS solution were used to ensure that all microbes  
63 were removed from the root surface. CARD-FISH on whole non-sonicated roots and thrice sonicated  
64 roots was used to analyze the efficacy of this procedure for removing microbes from the rhizoplane (Fig.  
65 S3). The sonicated roots were then stored at -80°C until DNA extraction the same day.

66       Bulk soil samples were collected from unplanted pots approximately 2 inches below the soil  
67 surface. The samples were placed in 15 ml tubes and stored at 4°C until DNA extraction the same day.

68       Samples for the field experiment were collected over a two-day period. The roots of plants in the  
69 field were collected with a bulb planter (Fiskars). The soil was shaken off the roots to leave ~1mm of soil  
70 still attached. These roots were placed in sterile PBS solution and brought back to the laboratory for  
71 isolation of the rhizocompartments as described above. Each rhizocompartment was isolated from each  
72 plant sampled and had total DNA extracted.

73 **DNA Extraction from Rhizocompartments**

74       The rhizosphere soil was concentrated by pipetting 1mL of the PBS / rhizosphere soil into a 2mL  
75 tube and centrifuging for 30 seconds at 10,000 g. The supernatant was discarded leaving only the soil  
76 fraction behind. The rhizoplane compartment was concentrated in the same manner, except all 15mL of

77 the sample was concentrated in the same 2 mL tube using multiple centrifugations. The endosphere  
78 fraction was pre-homogenized before the DNA extraction by bead beating for 1 minute (Mini Beadbeater,  
79 Biospec Products). The DNA for each sample was then extracted using the MoBio PowerSoil DNA  
80 isolation kit and eluted in 50  $\mu$ L of elution buffer. The rhizoplane samples typically had low DNA yield  
81 and were subsequently concentrated in a speedvac down to 10  $\mu$ L.

82 **16S rRNA gene V4 amplification, quantitation, and sequencing**

83 Targeted metagenomic profiling of the samples was carried out by sequencing the V4 region of  
84 the 16S rRNA gene. V4 amplification was carried out using primers modified from Caporaso et al, 2010  
85 (4). Briefly, these primers are designed to amplify from 515 to 806 of the 16S rRNA gene and they  
86 include a barcode an adaptor for annealing to the Illumina flow cell. Our primers differed in that both the  
87 primers contained a 12bp barcode instead of only the reverse primer (Dataset S25). This allowed us to  
88 pool many samples together using unique barcode combinations instead of relying on a multitude of  
89 reverse primers with unique barcodes. PCR reaction mixes were made using Qiagen HotStar HiFidelity  
90 polymerase. Each mix was done in a volume of 25  $\mu$ L using 14  $\mu$ L H<sub>2</sub>O, 5  $\mu$ L HotStar PCR Buffer, 2.5  
91  $\mu$ L forward primer (10  $\mu$ M), 2.5  $\mu$ L reverse primer (10  $\mu$ M), 1  $\mu$ L sample DNA, and 0.5  $\mu$ L HotStar  
92 polymerase. We used a touchdown PCR program on a Biometra TProfessional Basic Gradient  
93 thermocycler: 95°C for 5 min, then 7 cycles of 95°C for 45 sec, 65°C for 1 min (decreasing at 2°C /  
94 cycle), and 72°C for 90 sec, followed by 30 cycles of 95°C for 45 sec, 50°C for 30 sec, and 72°C for 90  
95 sec. A final extension at 72°C was used for 10 min and the reactions were held at 4°C. The reactions  
96 were run on a 1% agarose gel in order to ensure the amplification was successful. Unsuccessful reactions  
97 were attempted once more, but removed from the experiment if unsuccessful a second time.

98 The amplicons libraries were diluted 40x and quantified using an Agilent Bioanalyzer for the  
99 greenhouse libraries, or a Caliper LabChip GX for the field experiment libraries at the DNA Technologies  
100 Core at the Genome Center, UC Davis. The libraries were then pooled at equimolar concentrations into 4  
101 pooled libraries (2 libraries for the greenhouse experiment and 2 libraries for the field experiment). To  
102 remove any primer dimer from the pooled amplicon libraries we ran the 4 pooled libraries on 1.8%

103 agarose gels and extracted a 400 bp band. The bands were purified (Macherey-Nagel Nucleospic Gel and  
104 PCR Cleanup kit) and bioanalyzed as a final quality control check. Each library was submitted to the UC  
105 Davis DNA Technologies core for 250 x 250 paired end, dual index sequencing on an Illumina MiSeq  
106 instrument.

107 **Sequence Analysis**

108 The sequences obtained from the MiSeq runs were demultiplexed based on the barcode sequences  
109 using a custom Perl script based upon exact matching. The sequences were overlapped to form  
110 contiguous reads using MOTHUR's command make.contigs (5). Reads containing any ambiguous bases  
111 were then discarded along with any reads that were over 275 bp. The sequences were then clustered into  
112 operational taxonomic units (OTUs) by UCLUST (6) based on 97% pairwise identity using QIIME's (7)  
113 open reference OTU picking strategy which used the Greengenes 16S rRNA database (13\_5 release) as a  
114 reference (8). Taxonomic classification of the representative sequence for each OTU was done using  
115 QIIME's version of the Ribosomal Database Project's classifier (9) against the Greengenes 16S rRNA  
116 database (13\_5 release) using default parameters. All OTUs identified as belonging to chloroplast and  
117 mitochondria were removed from the data set. The representative sequences for each OTU were aligned  
118 using PyNAST (10) in QIIME. Chimeric OTUs were identified using QIIME's implementation of  
119 ChimeraSlayer (11) and removed from the OTU table and OTU representative sequences file. A  
120 phylogenetic tree was generated from the alignment file by FastTree (12).

121 **Statistical Analysis**

122 The resulting OTU table was divided by experiment and analyzed separately except when  
123 comparing methanogenic and methanotrophic OTUs. Low abundance OTUs were eliminated from the  
124 OTU table if they did not have a total of at least 5 counts across all the samples in the experiment.. OTU  
125 tables for each experiment were normalized by the trimmed mean of M values (TMM) method using the  
126 BioConductor package EdgeR in R (13). Weighted and Unweighted UniFrac (14) distances were  
127 calculated from the normalized OTU tables for each experiment.  $\alpha$ -diversity measurements were  
128 calculated by the function diversity() using the "Shannon" method in the R package Vegan (15).

129 Rarefaction curves were calculated using custom R scripts. Principal coordinate analyses utilizing the  
130 weighted and unweighted UniFrac distances were calculated using the pcoa() function from the R  
131 package Ape (16). CAP analysis was performed using the function capscale() from the R Package Vegan.  
132 When specifying CAP models, we constrained the analysis to the factor of interest while controlling for  
133 all other experimental factors and technical factors (MiSeq runs). Variance partitioning and significances  
134 for experimental factors was performed by running Vegan's permutest() function over the CAP model  
135 using a maximum of 500 permutations. Bulk soil samples were omitted from the CAP analysis when  
136 analyzing the greenhouse data. This was done because the bulk soil samples provided a confounding  
137 level within the *Cultivar* factor. Additionally, permutational MANOVA was carried out to using Vegan's  
138 function adonis() to measure effect size and significances on  $\beta$ -diversity. Differentially abundant OTUs  
139 were detected using EdgeR's generalized linear model (GLM) approach. This approach allows the user to  
140 test for differential OTU abundance between different levels of factors by employing a design matrix to  
141 account for complex experimental designs.

#### 142 **Co-abundance network analysis**

143 Only OTUs that were determined to be differentially abundant in experimental factors  
144 encompassed in the field experiment were used for network analysis, thus subsetting the data to OTUs  
145 with high variance (10,848 OTUs). Pairwise Pearson correlations were calculated between the remaining  
146 OTUs. The Pearson correlations were used as a distance metric to build a hierarchically clustered  
147 dendrogram using average linkage. The dendrogram was dynamically pruned using the R package  
148 'dynamicTreeCut' (17). This tree cutting technique was employed due to its ability to detect nested  
149 clusters within larger clusters. A hypergeometric test was used to detect taxonomies that were  
150 significantly enriched in specific clusters. Taxonomies were queried for their involvement in methane  
151 metabolism and cycling using the BioCyc (18), MetaCyc (18), or KEGG Pathway (19) databases unless  
152 otherwise noted.

#### 153 **CARD-FISH**

154 Roots designated for CARD-FISH were fixed using 4% formaldehyde in PBS for 4 hours,

155 washed twice with PBS, and stored in 1:1 ethanol:PBS at 4° C. CARD-FISH treatments were done in  
156 accordance with previous studies in *Arabidopsis* (2, 3, 20) using the eubacterial probe Eub338 (5'-  
157 GCTGCCTCCCGTAGGAGT-3', 35% formamide, Biomers Ulm, Germany) and its nonsense sequence  
158 as a negative control, NON338 (5' - ACTCCTACGGGAGGCAGC-3', 30% formamide) labeled with  
159 horseradish peroxidase at the 5' end (Biomers Ulm, Germany). Signal amplification was carried out  
160 using fluorescently labeled tyramide (Fluorescent solutions). All microscopy images were taken using a  
161 confocal laser scanning microscope in the Department of Plant Biology at UC Davis (Zeiss LSM 710).

162 **Amplification, cloning, and sequencing of *mcrA*.**

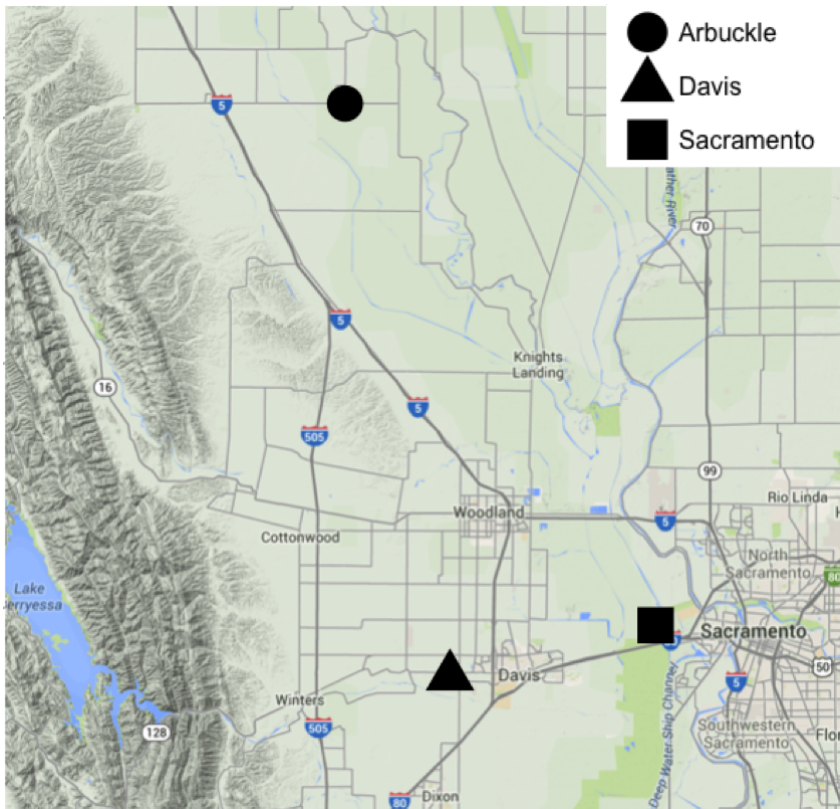
163 Total community DNA extracted from rhizosphere and endosphere samples from the DS RR field  
164 was used as a template to amplify fragments of the *mcrA* gene. PCR was performed following the  
165 protocol described in Juottonen et al. (21) using the primers designed in Springer et al. (22) The amplified  
166 products were cloned with the TOPO TA cloning kit (Invitrogen), and plasmid DNA was recovered from  
167 47 clones (29 from endosphere samples and 18 from rhizosphere samples) using GeneJET plasmid  
168 miniprep kit (Thermo Scientific). The cloned fragments were sequenced by the UC Davis Sequencing  
169 Facility using the M13 primers. A BLAST search was performed using the NCBI nucleotide database,  
170 and the top alignment was reported for each sequence (alignments without a defined taxonomy were  
171 excluded).

172 **References**

- 173 1. Bulgarelli D, Schlaeppi K, Spaepen S, van Themaat EVL, & Schulze-Lefert P (2013) Structure  
174 and functions of the bacterial microbiota of plants. *Annual review of plant biology* 64:807-838.
- 175 2. Bulgarelli D, et al. (2012) Revealing structure and assembly cues for *Arabidopsis* root-  
176 inhabiting bacterial microbiota. *Nature* 488(7409):91-95.
- 177 3. Lundberg DS, et al. (2012) Defining the core *Arabidopsis thaliana* root microbiome. *Nature*  
178 488(7409):86-90.
- 179 4. Caporaso JG, et al. (2011) Global patterns of 16S rRNA diversity at a depth of millions of  
180 sequences per sample. *Proceedings of the National Academy of Sciences* 108(Supplement  
181 1):4516-4522.
- 182 5. Schloss PD, et al. (2009) Introducing mothur: open-source, platform-independent, community-  
183 supported software for describing and comparing microbial communities. *Applied and  
184 environmental microbiology* 75(23):7537-7541.

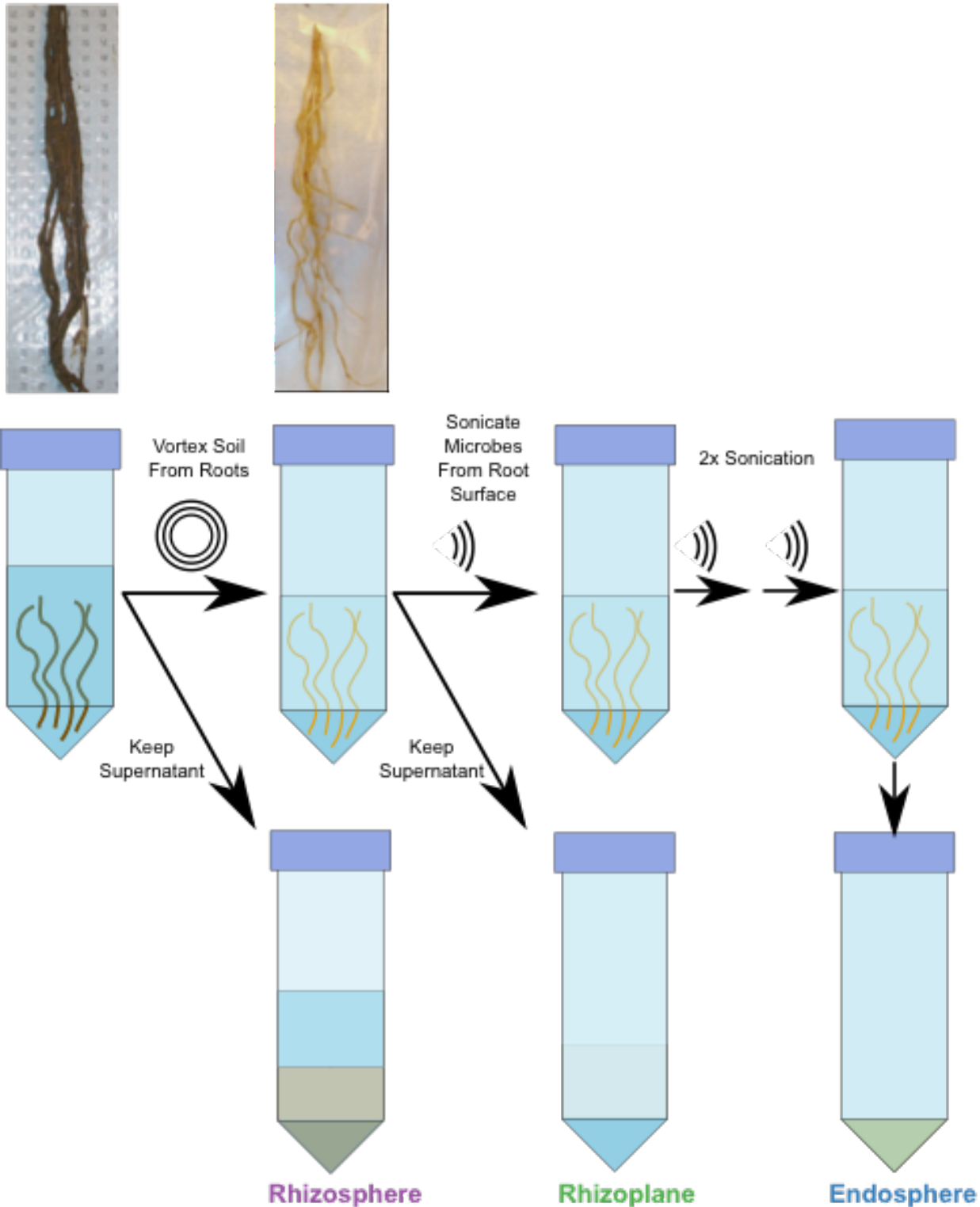
- 186 6. Edgar RC (2010) Search and clustering orders of magnitude faster than BLAST.  
187 *Bioinformatics* 26(19):2460-2461.
- 188 7. Caporaso JG, et al. (2010) QIIME allows analysis of high-throughput community sequencing  
189 data. *Nature methods* 7(5):335-336.
- 190 8. DeSantis TZ, et al. (2006) Greengenes, a chimera-checked 16S rRNA gene database and  
191 workbench compatible with ARB. *Applied and environmental microbiology* 72(7):5069-  
192 5072.
- 193 9. Cole JR, et al. (2009) The Ribosomal Database Project: improved alignments and new tools  
194 for rRNA analysis. *Nucleic acids research* 37(suppl 1):D141-D145.
- 195 10. Caporaso JG, et al. (2010) PyNAST: a flexible tool for aligning sequences to a template  
196 alignment. *Bioinformatics* 26(2):266-267.
- 197 11. Haas BJ, et al. (2011) Chimeric 16S rRNA sequence formation and detection in Sanger and  
198 454-pyrosequenced PCR amplicons. *Genome research* 21(3):494-504.
- 199 12. Price MN, Dehal PS, & Arkin AP (2009) FastTree: computing large minimum evolution trees  
200 with profiles instead of a distance matrix. *Molecular biology and evolution* 26(7):1641-  
201 1650.
- 202 13. Robinson MD, McCarthy DJ, & Smyth GK (2010) edgeR: a Bioconductor package for  
203 differential expression analysis of digital gene expression data. *Bioinformatics* 26(1):139-  
204 11.
- 205 14. Lozupone C & Knight R (2005) UniFrac: a new phylogenetic method for comparing  
206 microbial communities. *Applied and environmental microbiology* 71(12):8228-8235.
- 207 15. Oksanen J, et al. (2007) The vegan package. *Community ecology package*.
- 208 16. Paradis E, Claude J, & Strimmer K (2004) APE: analyses of phylogenetics and evolution in R  
209 language. *Bioinformatics* 20(2):289-290.
- 210 17. Langfelder P, Zhang B, & Horvath S (2008) Defining clusters from a hierarchical cluster tree:  
211 the Dynamic Tree Cut package for R. *Bioinformatics* 24(5):719-720.
- 212 18. Caspi R, et al. (2008) The MetaCyc Database of metabolic pathways and enzymes and the  
213 BioCyc collection of Pathway/Genome Databases. *Nucleic acids research* 36(suppl  
214 1):D623-D631.
- 215 19. Kanehisa M & Goto S (2000) KEGG: kyoto encyclopedia of genes and genomes. *Nucleic  
216 acids research* 28(1):27-30.
- 217 20. Eickhorst T & Tippkötter R (2008) Improved detection of soil microorganisms using  
218 fluorescence *in situ* hybridization (FISH) and catalyzed reporter deposition (CARD-  
219 FISH). *Soil Biology and Biochemistry* 40(7):1883-1891.
- 220 21. Juutonen H, Galand PE, & Yrjälä K (2006) Detection of methanogenic Archaea in peat:  
221 comparison of PCR primers targeting the *mcrA* gene. *Research in microbiology*  
222 157(10):914-921.
- 223 22. Springer E, Sachs MS, Woese CR, & Boone DR (1995) Partial gene sequences for the A  
224 subunit of methyl-coenzyme M reductase (*mcrI*) as a phylogenetic tool for the family  
225 Methanosarcinaceae. *International Journal of Systematic Bacteriology* 45(3):554-559.
- 226
- 227
- 228
- 229
- 230

231 **Supplementary Figures**



232

233 **Fig. S1 Map depicting soil collection locations for greenhouse experiment.**



234

235 **Fig. S2. Sampling and collection of the rhizocompartments.** Roots are collected from rice  
236 plants and soil is shaken off the roots to leave ~1mm of soil around the roots. The ~1 mm of soil

237 is washed off in PBS and kept as the rhizosphere compartment. The clean roots are then washed  
238 twice more to remove remaining soil and placed into clean PBS in a 50 mL Falcon tube. The  
239 rhizoplane microbes are extracted by sonicating the roots with the rhizosphere compartment  
240 removed. The sonicated roots are then placed in a new, clean Falcon tube and sonicated twice  
241 more, decanting the PBS in the tube between sonications and refilling with clean PBS. These  
242 roots are then kept for extracting the endospheric microbes.

243

244

245

246

247

248

249

250

251

252

253

254

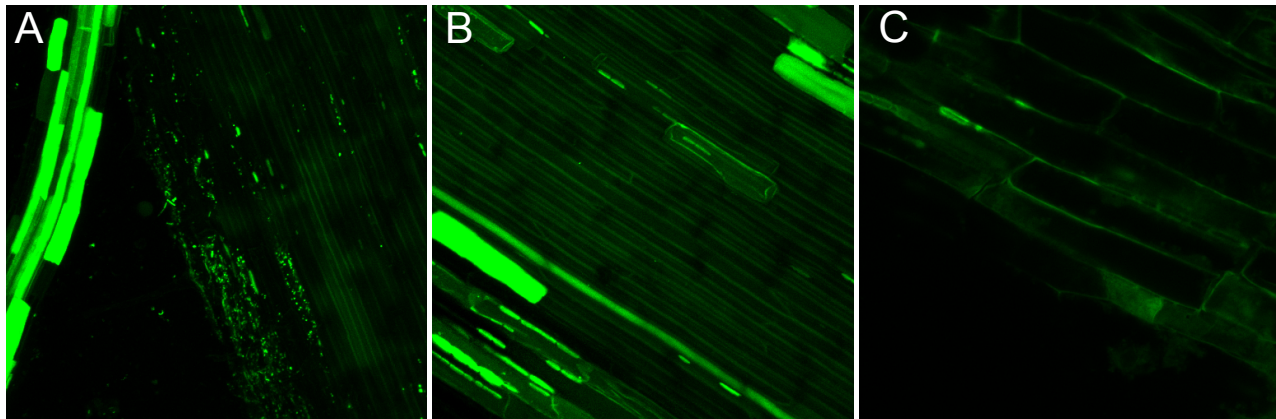
255

256

257

258

259



260

261 **Fig. S3. CARD-FISH reveals that rhizoplane microbes are removed after sonication of rice  
262 roots. (A) Pre-sonicated root incubated with the Eub338 eubacterial probe. (B) Thrice sonicated  
263 root incubated with the Eub338 eubacterial probe. (C) Pre-sonicated root probed with the  
264 antisense Eub338 probe as a negative control. Files of root cells showing bright signals are  
265 presumed to be dead cells damaged during the removal of rhizosphere soil.**

266

267

268

269

270

271

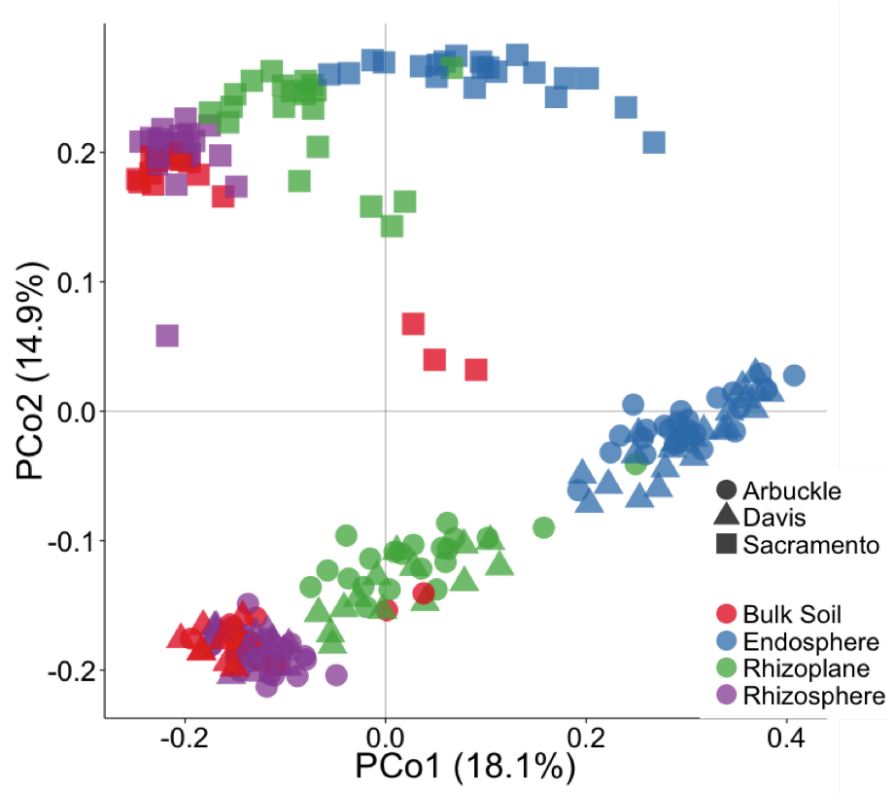
272

273

274

275

276



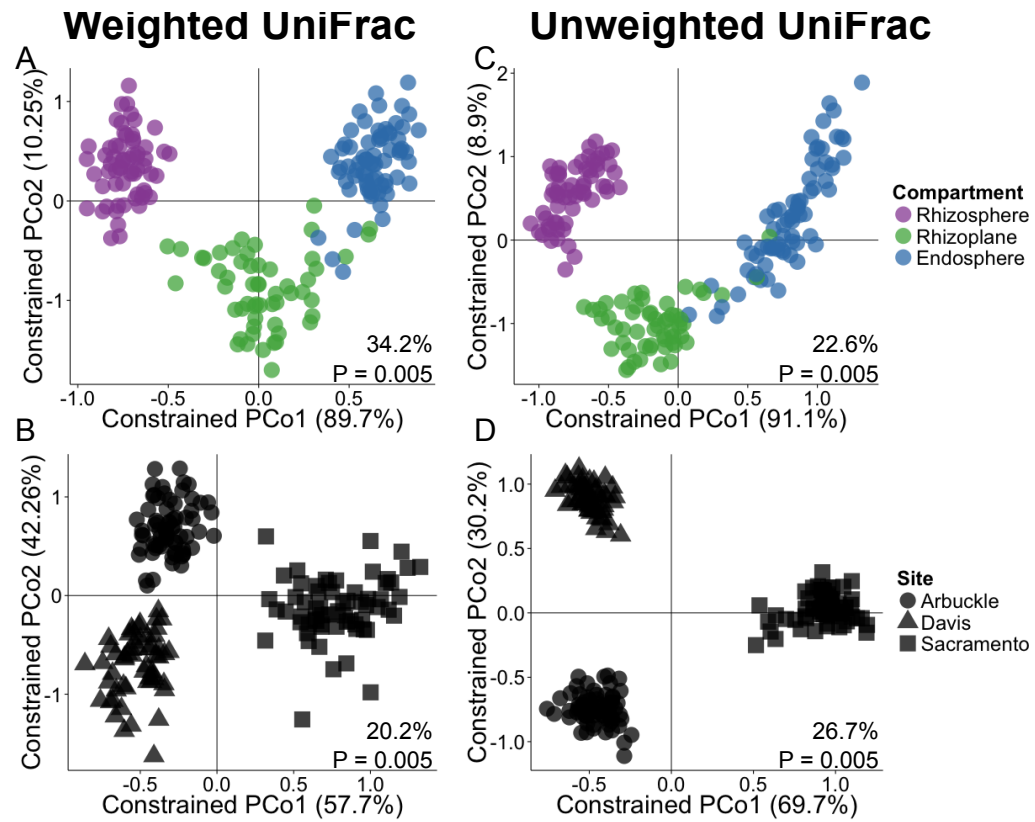
277

278 **Fig. S4. Rice root-associated microbiomes vary by rhizocompartment and site in the**  
 279 **greenhouse experiment.** PCoA using the unweighted UniFrac distance metric indicates that  
 280 microbiomes separate by rhizocompartment and soil source.

281

282

283

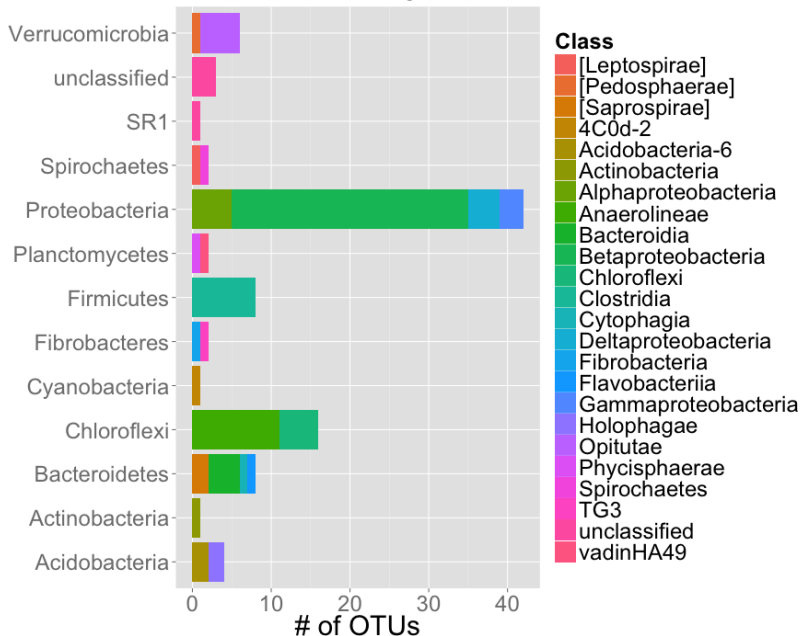


284

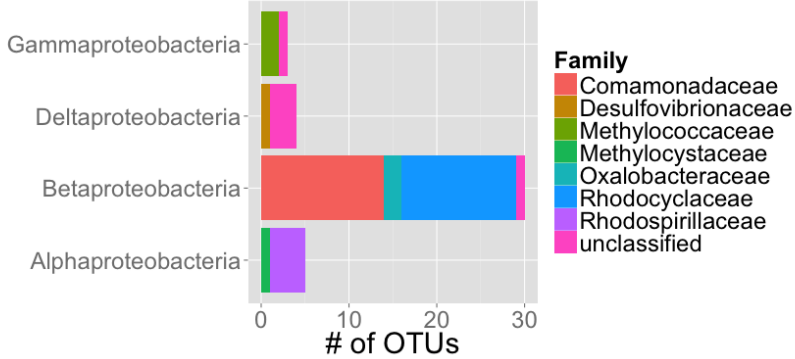
285 **Fig. S5. CAP analysis confirms that rice root microbiomes vary by compartment and soil  
286 source. (A)** CAP analysis ordination constrained to rhizocompartment and conditioned on soil  
287 source, cultivar, and technical factors using the weighted UniFrac distance metric. **(B)** CAP  
288 analysis ordination constrained to soil source and conditioned on rhizocompartment, cultivar,  
289 and technical factors using the weighted UniFrac distance metric. **(C)** CAP analysis ordination  
290 constrained to rhizocompartment and conditioned on soil source, cultivar, and technical factors  
291 using the unweighted UniFrac distance metric. **(D)** CAP analysis ordination constrained to soil  
292 source and conditioned on rhizocompartment, cultivar, and technical factors using the weighted  
293 UniFrac distance metric. All variances attributable to the constrained factor and the significance  
294 of the factor are portrayed in each plot.

295

A

**All Phyla**

B

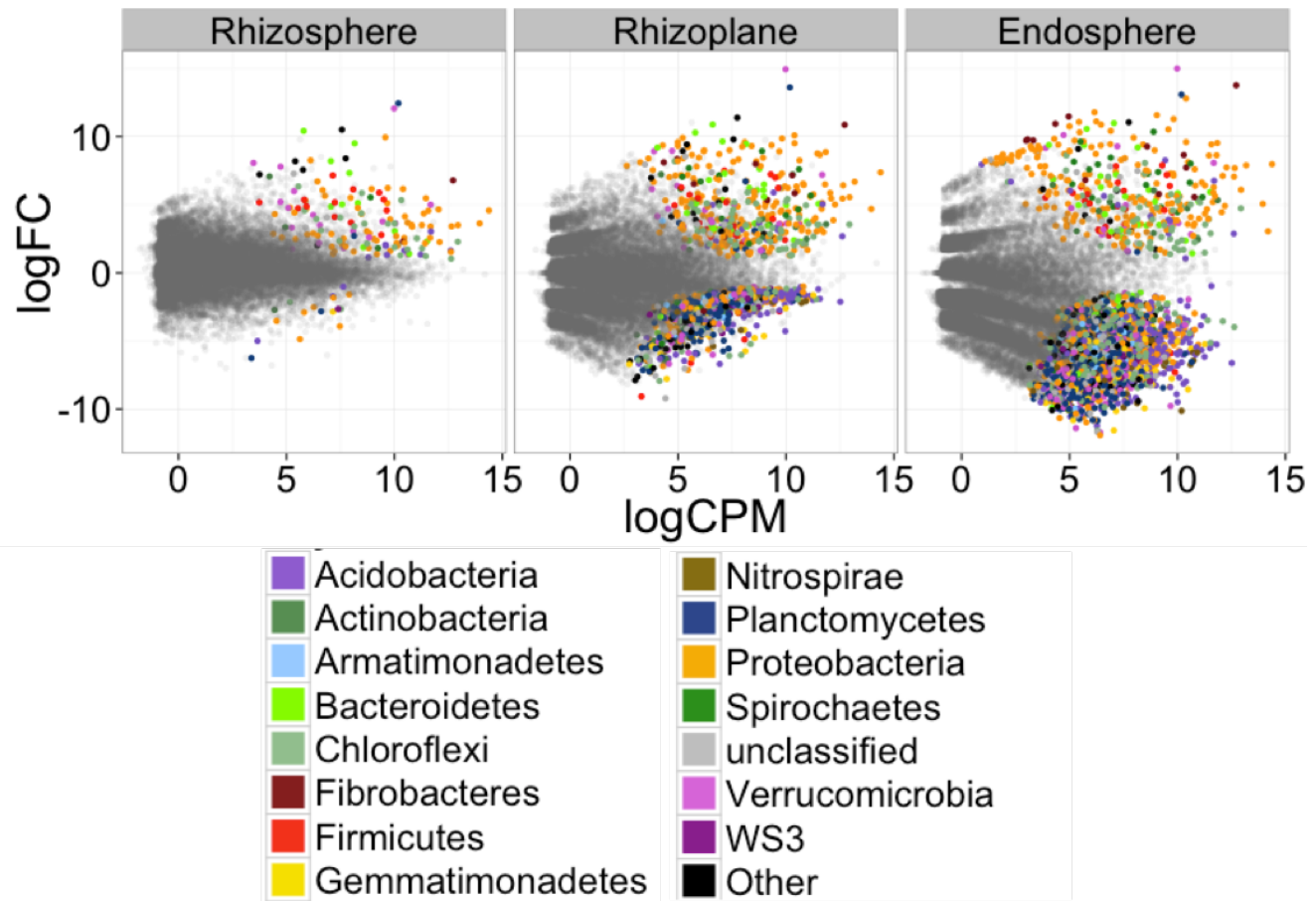
**Proteobacteria**

296

**Fig. S6. A set of 96 OTUs mainly consisting of Proteobacteria is enriched across every compartment in the greenhouse experiment. (A) Number of OTUs and the phyla and classes they belong to that are enriched across all rhizocompartments in the greenhouse experiment. (B) A subset of the Proteobacteria and the classes and families they belong to in the OTUs that are enriched across all rhizocompartments in the greenhouse.**

302

303



304

305 **Fig. S7 Microbes enriched and depleted in the rhizocompartments compared to bulk soil**

306 **have taxonomic patterns.** Each point represents one OTU and the color of the point represents  
 307 the OTU's assigned Phyla.

308

309

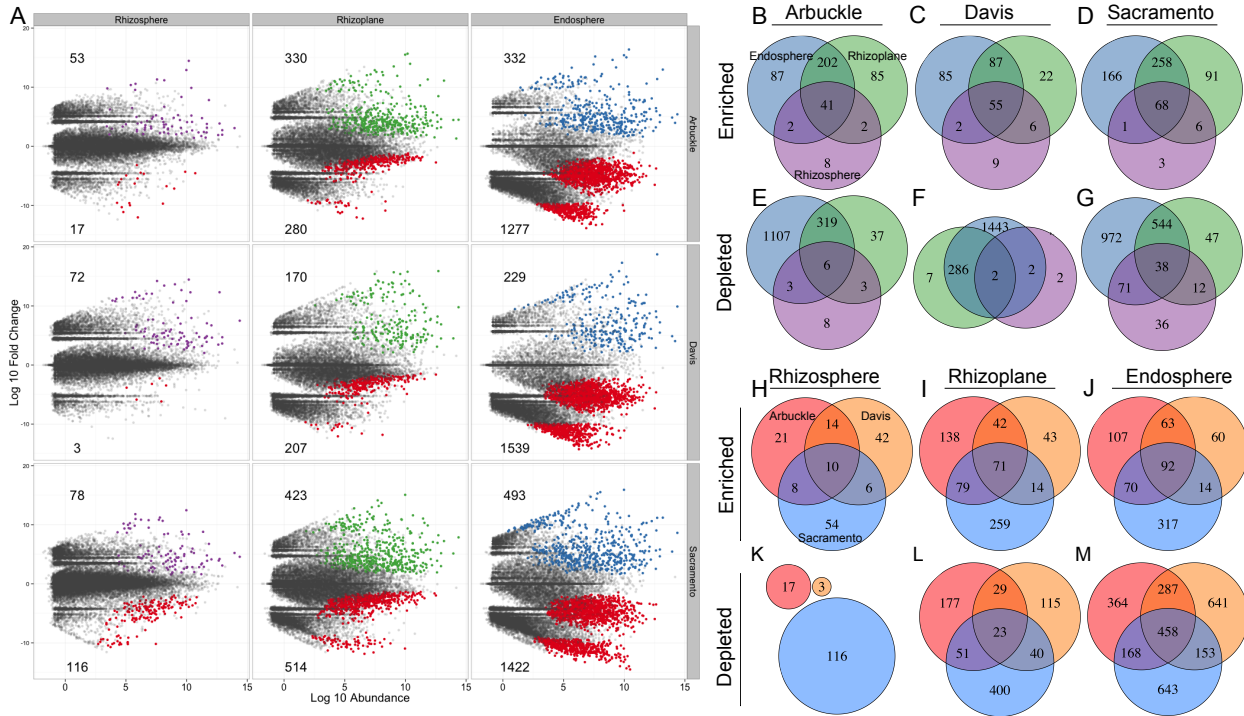
310

311

312

313

314



316 **Fig. S8. The different soil sources have commonalities and differences in differentially  
317 abundant OTUs.** (a) MVA plots representing enrichment and depletion of OTUs in each  
318 compartment compared to bulk soil across each soil source in the greenhouse experiment. (b) A  
319 venn diagram comparing differentially enriched OTUs in each compartment in Arbuckle soil. (c)  
320 A venn diagram comparing differentially enriched OTUs in each compartment in Davis soil. (d)  
321 A venn diagram comparing differentially enriched OTUs in each compartment in Sacramento  
322 soil. (e) A venn diagram comparing differentially depleted OTUs in each compartment in  
323 Arbuckle soil. (f) A venn diagram comparing differentially depleted OTUs in each compartment in  
324 Davis soil. (g) A venn diagram comparing differentially depleted OTUs in each compartment in  
325 Sacramento soil. (h) A venn diagram comparing differentially enriched OTUs in each soil for  
326 the rhizosphere compartment. (i) A venn diagram comparing differentially enriched OTUs in  
327 each soil for the rhizoplane compartment. (j) A venn diagram comparing differentially enriched  
328 OTUs in each soil for the endosphere compartment. (k) A venn diagram comparing differentially

329 depleted OTUs in each soil for the rhizosphere compartment. (**l**) A venn diagram comparing  
330 differentially depleted OTUs in each soil for the rhizoplane compartment. (**m**) A venn diagram  
331 comparing differentially depleted OTUs in each soil for the endosphere compartment. Coloration  
332 is consistent for rhizocompartments across (b) to (g) and consistent for soil sources across (h) to  
333 (m).

334

335

336

337

338

339

340

341

342

343

344

345

346

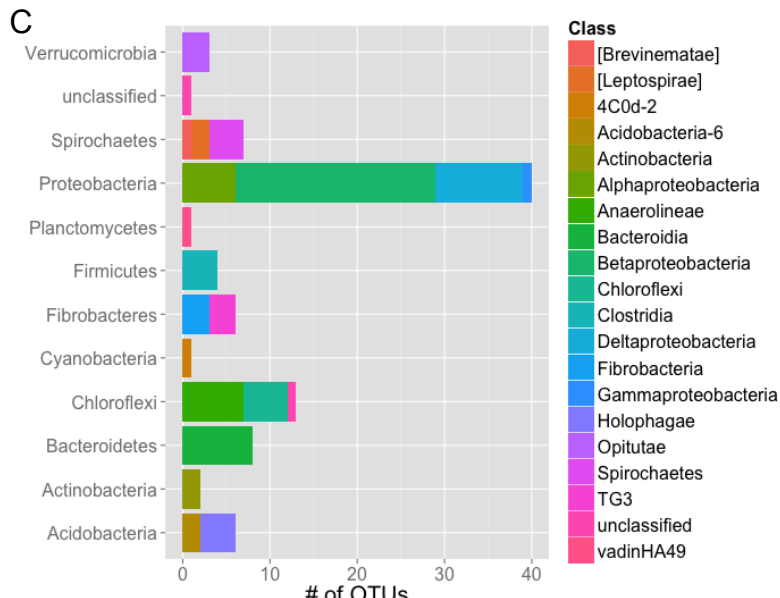
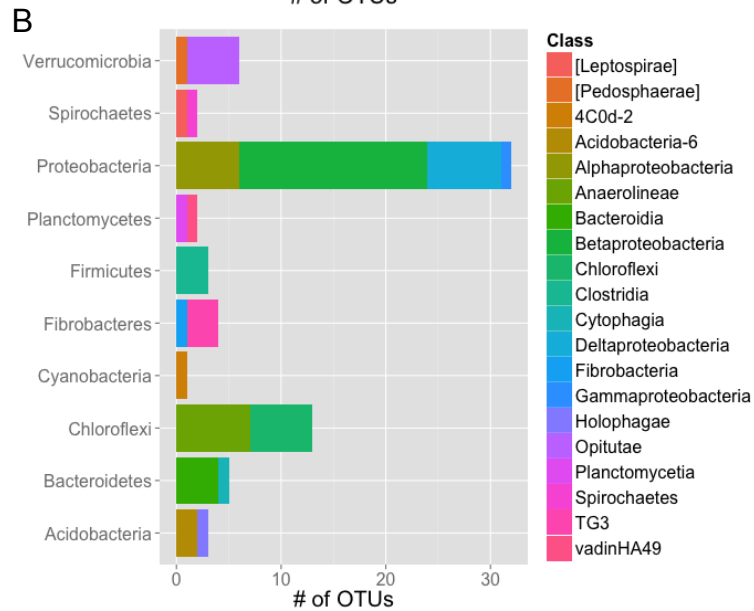
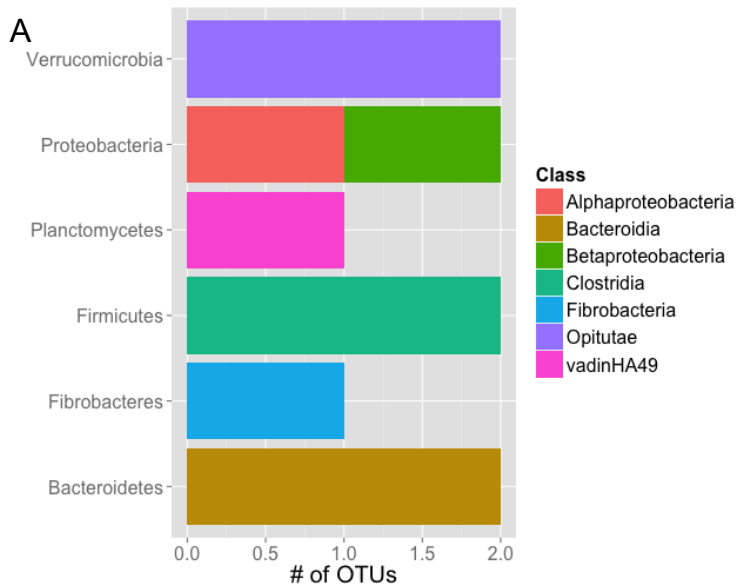
347

348

349

350

351



353 **Fig. S9.** Rice plants grown in diverse soil sources have commonalities in enriched OTUs in  
354 each rhizocompartment. Plants grown in Davis, Arbuckle, and Sacramento soil share enriched  
355 OTUs in the (A) rhizosphere, (B) rhizoplane, and (C) endosphere.

356

357

358

359

360

361

362

363

364

365

366

367

368

369

370

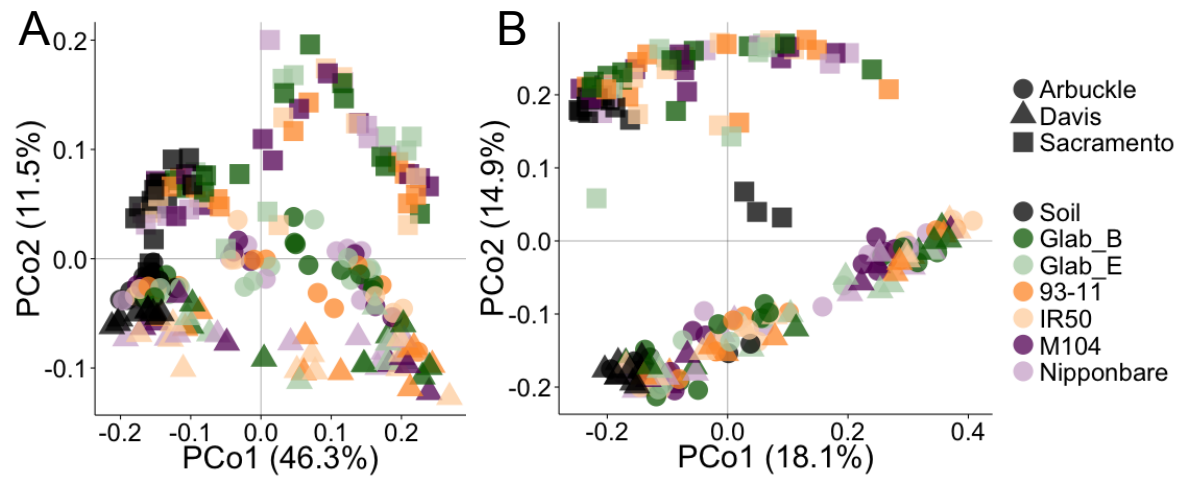
371

372

373

374

375



376

377 **Fig S10. Unconstrained PCoA reveals no distinct clustering of microbiomes of different rice**  
 378 **cultivars. (A)** Unconstrained PCoA using the weighted UniFrac distance metric. **(B)**  
 379 Unconstrained PCoA using the unweighted UniFrac distance metric.

380

381

382

383

384

385

386

387

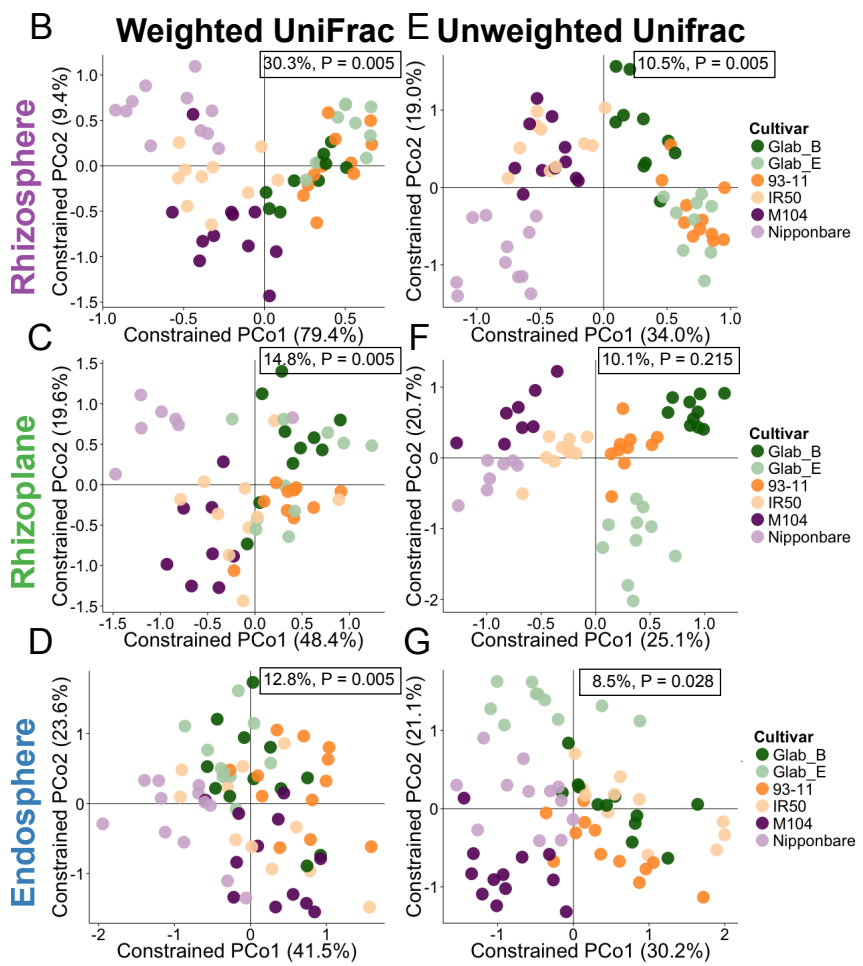
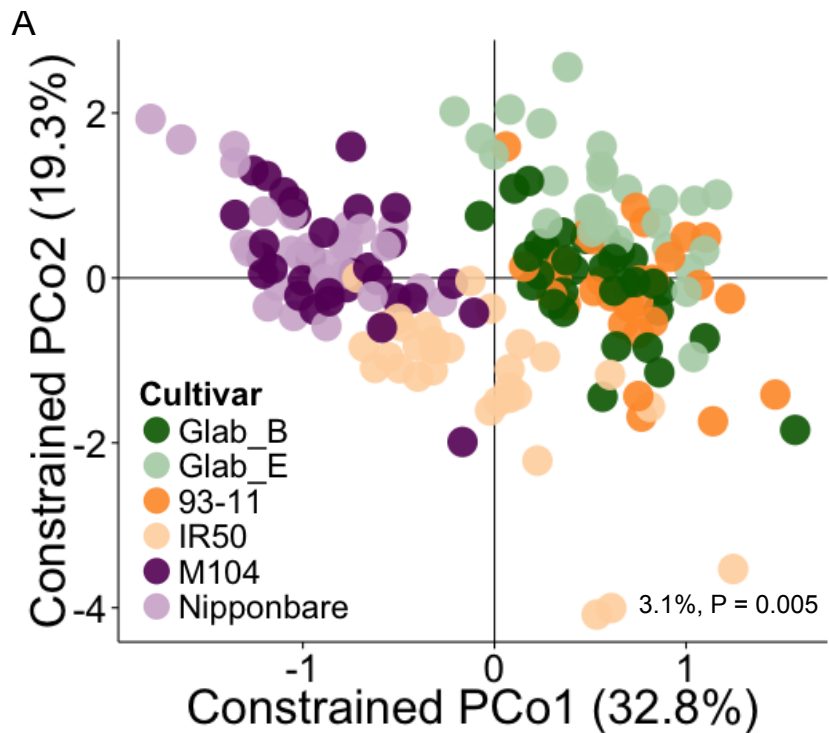
388

389

390

391

392



394 **Fig S11. CAP analysis constrained to rice cultivar while conditioning on**  
395 **rhizocompartment, soil source, and technical factors reveals distinct clustering patterns of**  
396 **microbiomes between rice genotypes.** (A) CAP analysis of the whole data using the  
397 unweighted UniFrac distance metric. (B - D) CAP analysis constrained to rice cultivar using the  
398 weighted UniFrac distance metric for (B) the rhizosphere samples, (C) the rhizoplane samples,  
399 (D) the endosphere samples. (E – G) CAP analysis constrained to rice cultivar using the  
400 unweighted distance metric for (E) the rhizosphere samples, (F) the rhizoplane samples, (G) the  
401 endosphere samples. All variances attributable to the constrained factor and the significance of  
402 the factor are portrayed in each plot.

403

404

405

406

407

408

409

410

411

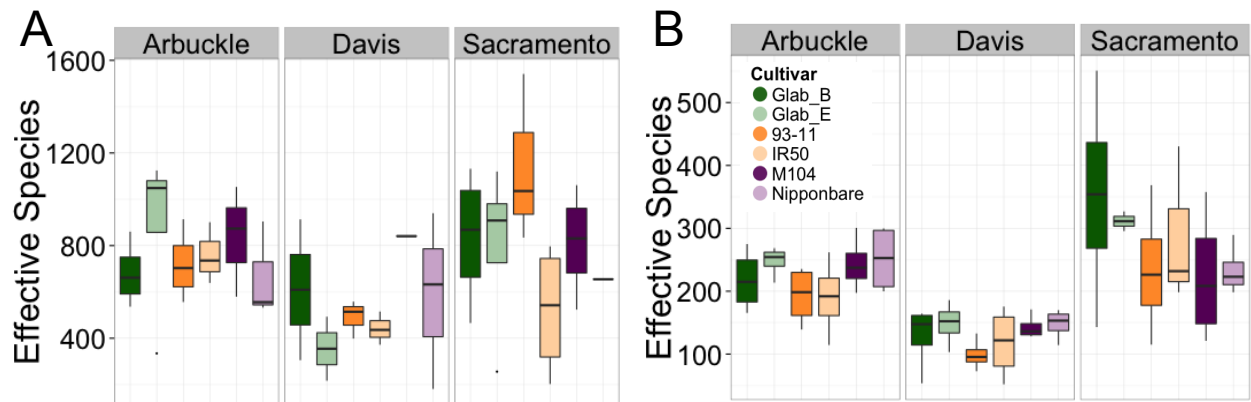
412

413

414

415

416



417

418 **Fig S12. Alpha diversities microbes on the rhizoplane and endosphere of rice cultivars**  
419 **grown in different show no genotypic patterns. (A) Rhizoplane alpha diversities. (B)**  
420 Endosphere alpha diversities.

421

422

423

424

425

426

427

428

429

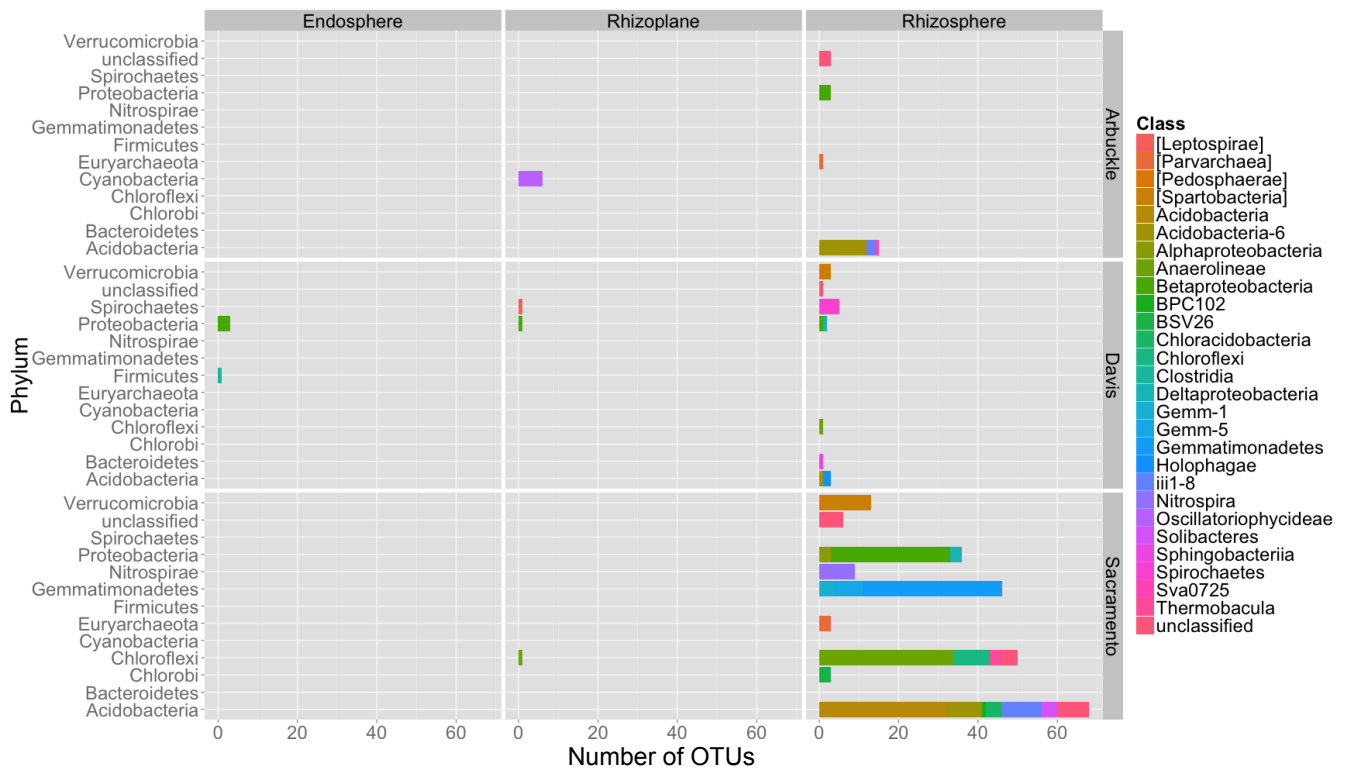
430

431

432

433

434



435

436 **Fig. S13. Differentially abundant OTUs between rice cultivars in each rhizocompartment  
437 and soil source.**

438

439

440

441

442

443

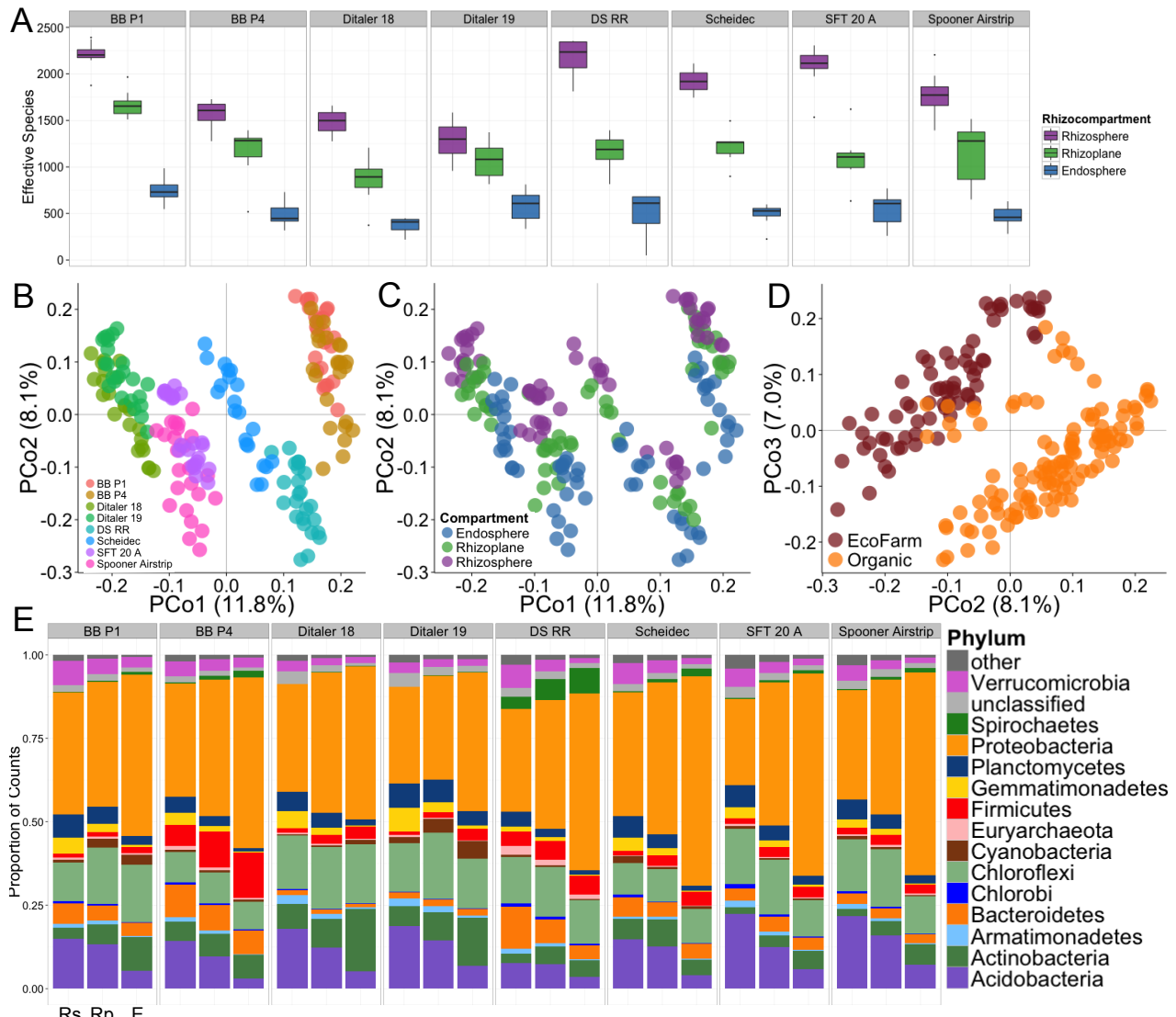
444

445

446

447

448

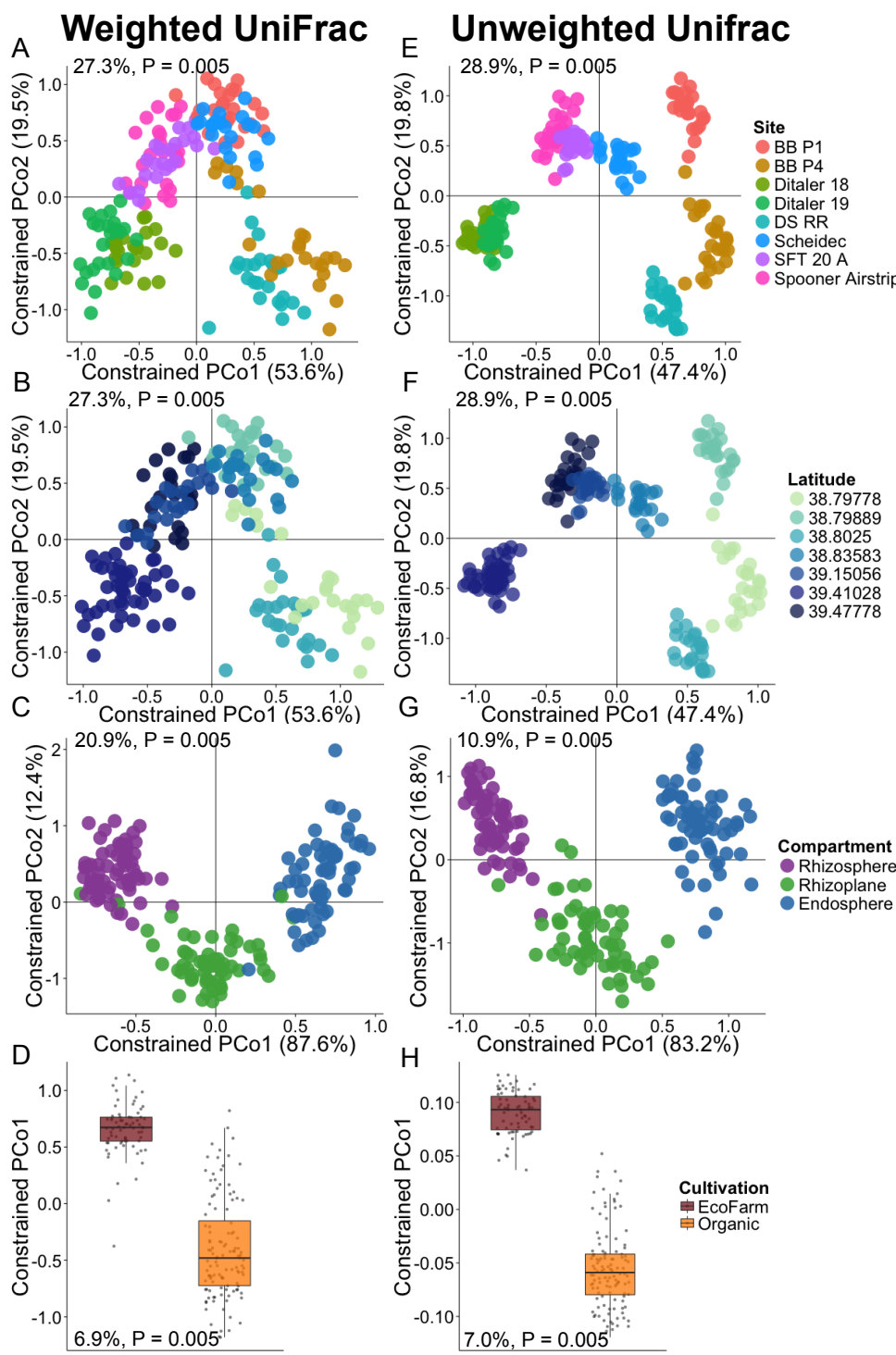


449 **Fig. S14. A gradient of diversity exists in the rhizocompartments of field grown rice. (a)**  $\alpha$ -  
450 diversity (Shannon) of all rhizocompartments sampled from all fields. **(b)** PCoA using the  
451 weighted UniFrac metric colored by field site. **(c)** Same PCoA and axes as represented in (b),  
452 colored by rhizocompartment. **(d)** Same PCoA represented in (b) and (c), axes 2 and 3 are shown  
453 and colored by cultivation practice. **(e)** Distribution of phyla across each rhizocompartment and  
454 every field. Rs, Rhizosphere; Rp Rhizoplane; E, Endosphere.

455

456

457



458

459 **Fig. S15. CAP analysis of the field data reveals that microbiomes vary by**  
 460 **rhizocompartment, field site, and cultivation practice. (A – D) CAP analysis using the**  
 461 **weighted UniFrac metric. (A) CAP analysis constrained to field site and conditioning on**

462 rhizocompartment, cultivation practice, and technical factors. **(B)** Same analysis as **(A)** but  
463 colored by latitude. **(C)** CAP analysis constrained to rhizocompartment conditioned on field site,  
464 cultivation practice, and technical factors. **(D)** CAP analysis on constrained to cultivation  
465 practice. **(E – H)** CAP analysis using the unweighted UniFrac metric. **(E)** CAP analysis  
466 constrained to field site and conditioning on rhizocompartment, cultivation practice, and  
467 technical factors. **(F)** Same analysis as **(E)** but colored by latitude. **(G)** CAP analysis constrained  
468 to rhizocompartment conditioned on field site, cultivation practice, and technical factors. **(H)**  
469 CAP analysis on constrained to cultivation practice. All variances attributable to the constrained  
470 factor and the significance of the factor are portrayed in each plot.

471

472

473

474

475

476

477

478

479

480

481

482

483

484

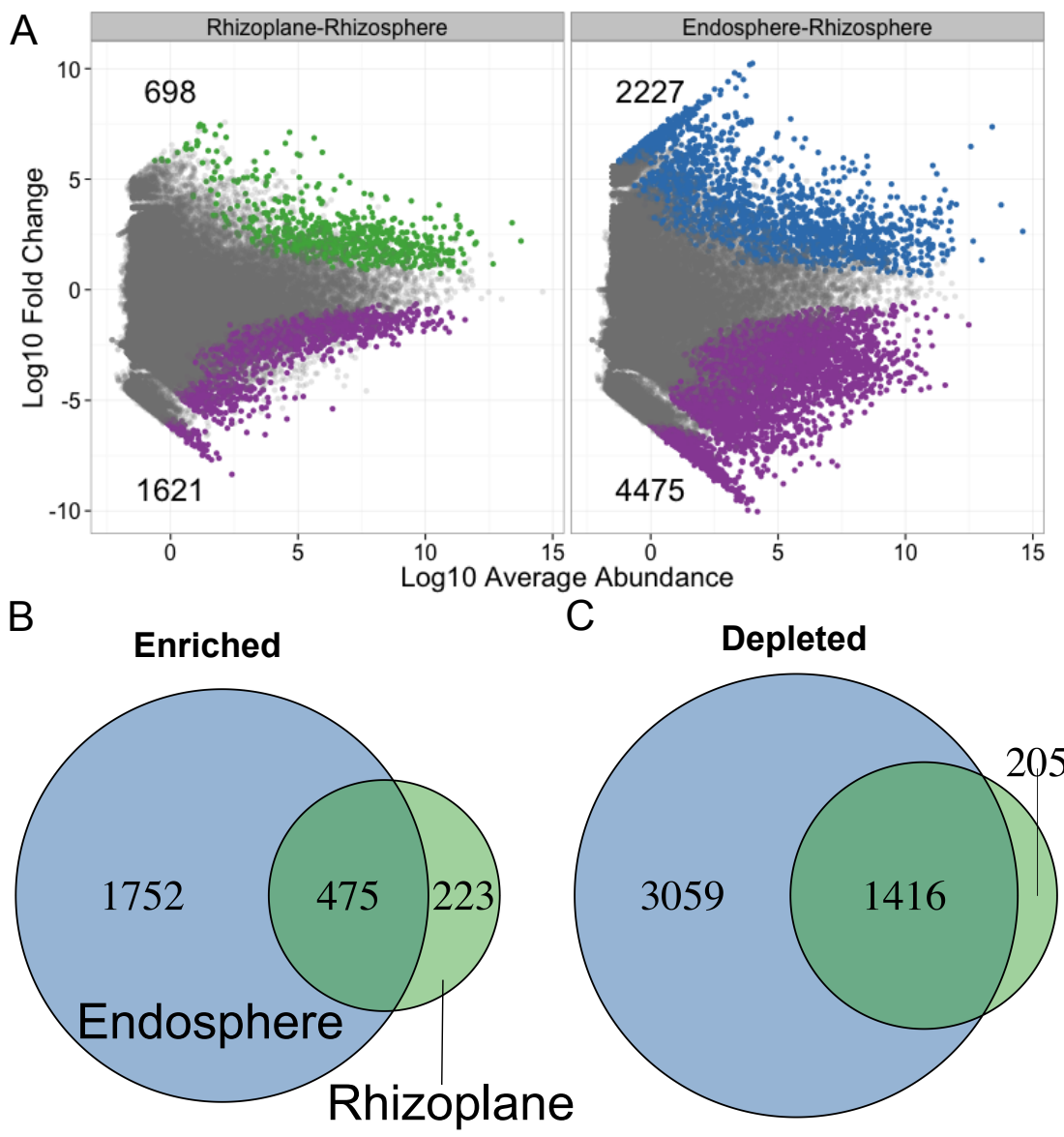
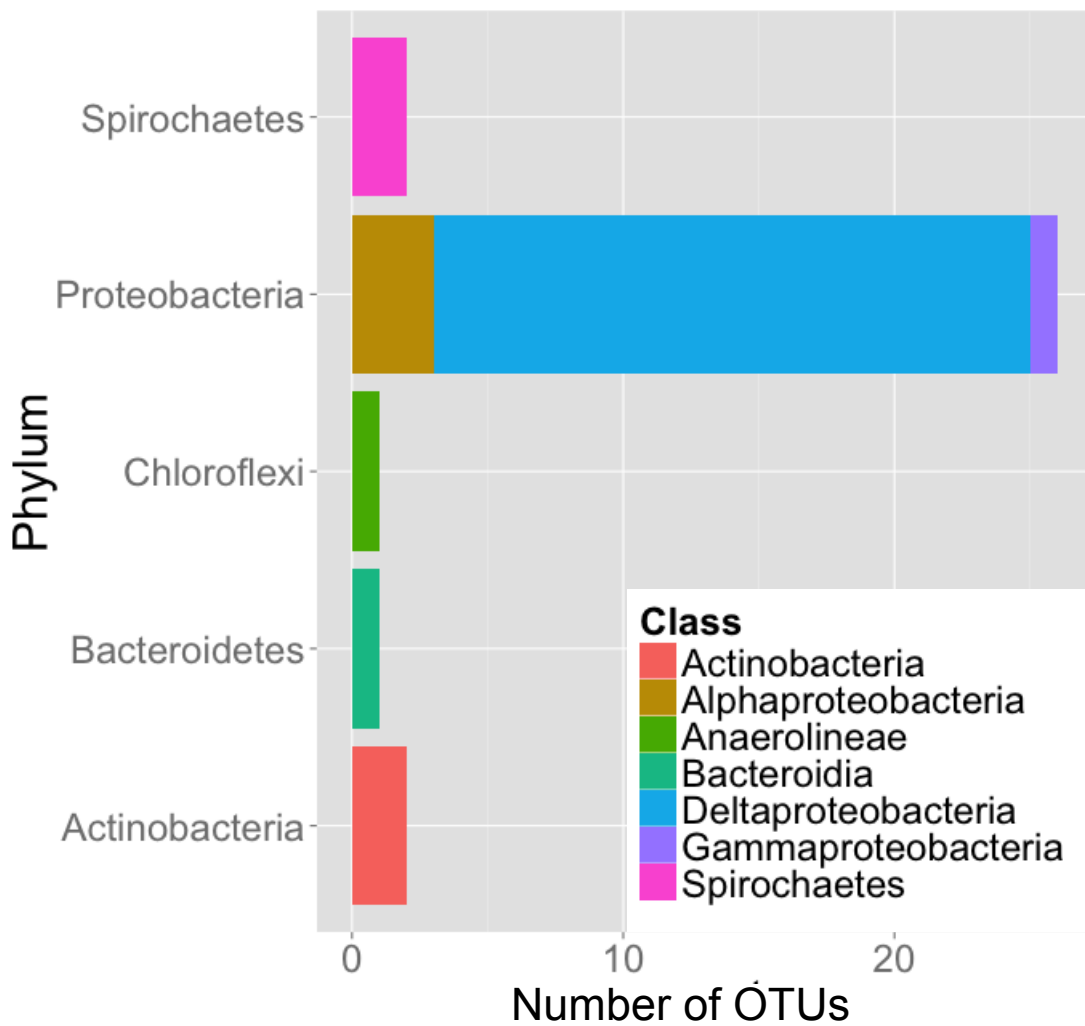


**Fig. S16. The rhizocompartments of field grown plants are enriched and depleted for OTUs.** (a) MVA plot displaying enriched OTUs in the endosphere and the rhizoplane compared to the rhizosphere. (b) Venn diagram displaying similarities and differences among significantly enriched OTUs in the rhizoplane and endosphere. (c) Venn diagram displaying the similarities and differences among significantly depleted OTUs in the rhizoplane and endosphere. The color scheme is consistent of the rhizocompartments in the venn diagrams.



493

494 **Fig. S17. A core endospheric microbiome consisting of 32 OTUs enriched across all field  
sites displayed by phylum and class.**

496

497

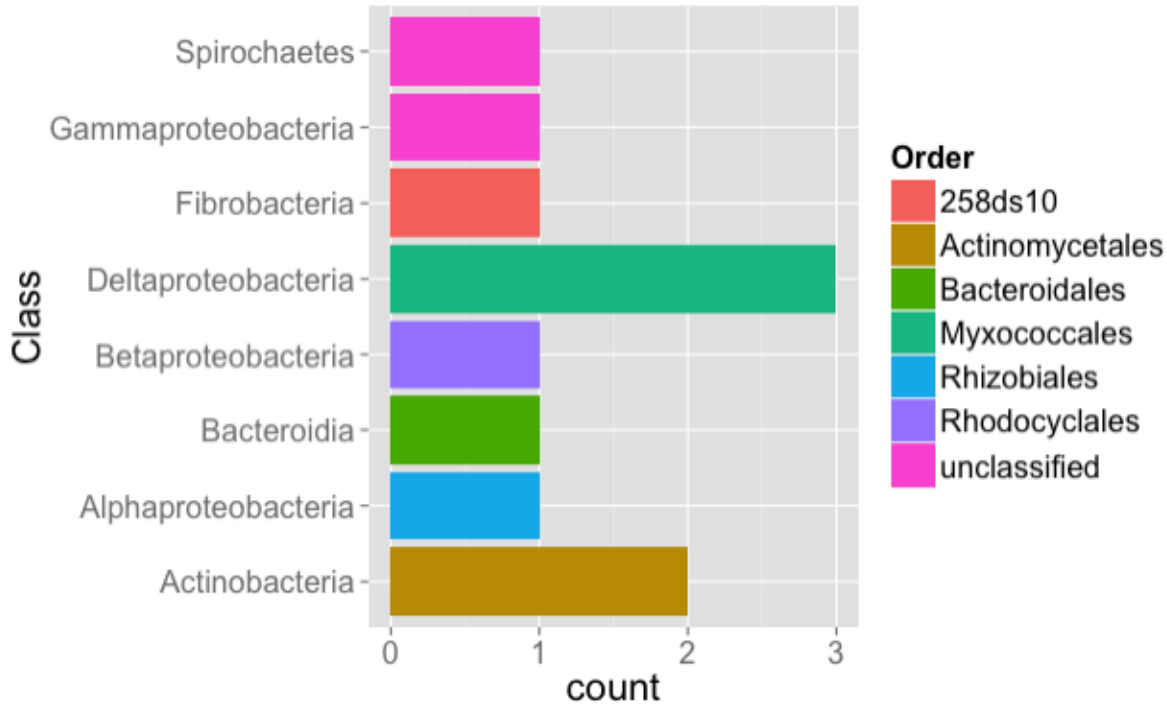
498

499

500

501

502



503

504 **Fig. S18 The greenhouse core endosphere enriched microbiome shares 11 OTUs with the**  
 505 **field enriched endosphere microbiome.**

506

507

508

509

510

511

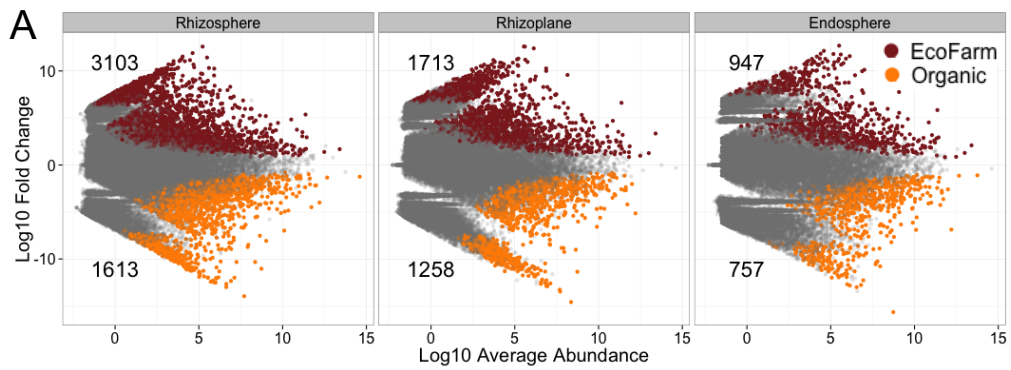
512

513

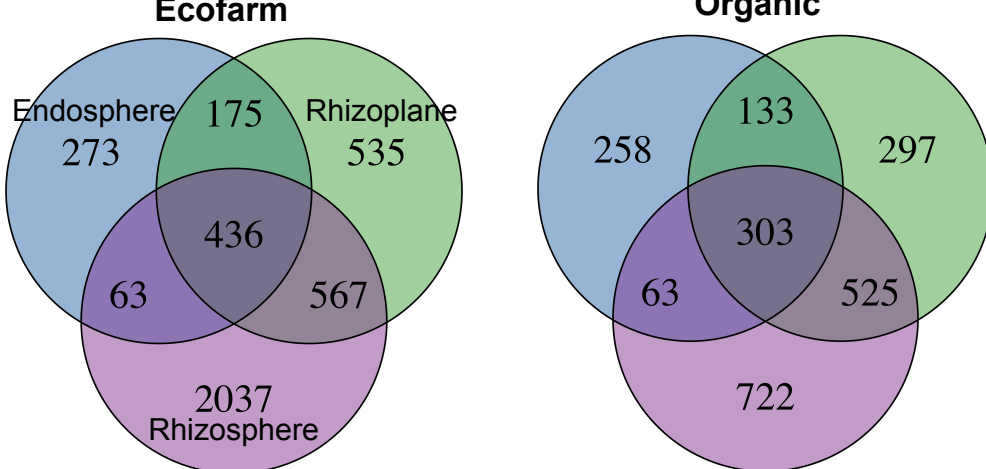
514

515

516



**B** **Ecofarm** **C** **Organic**



517

518 **Fig. S19. Differential OTU abundance between cultivation practices.** (a) MVA plot  
 519 displaying OTUs enriched in either organic or ecofarming practices across each  
 520 rhizocompartment. (b) Venn diagram indicating similarities of enriched OTUs between  
 521 rhizocompartments under ecofarm cultivation. (c) Venn diagram indicating similarities of  
 522 enriched OTUs between rhizocompartments under organic cultivation. The color scheme is  
 523 consistent of the rhizocompartments in the venn diagrams.

524

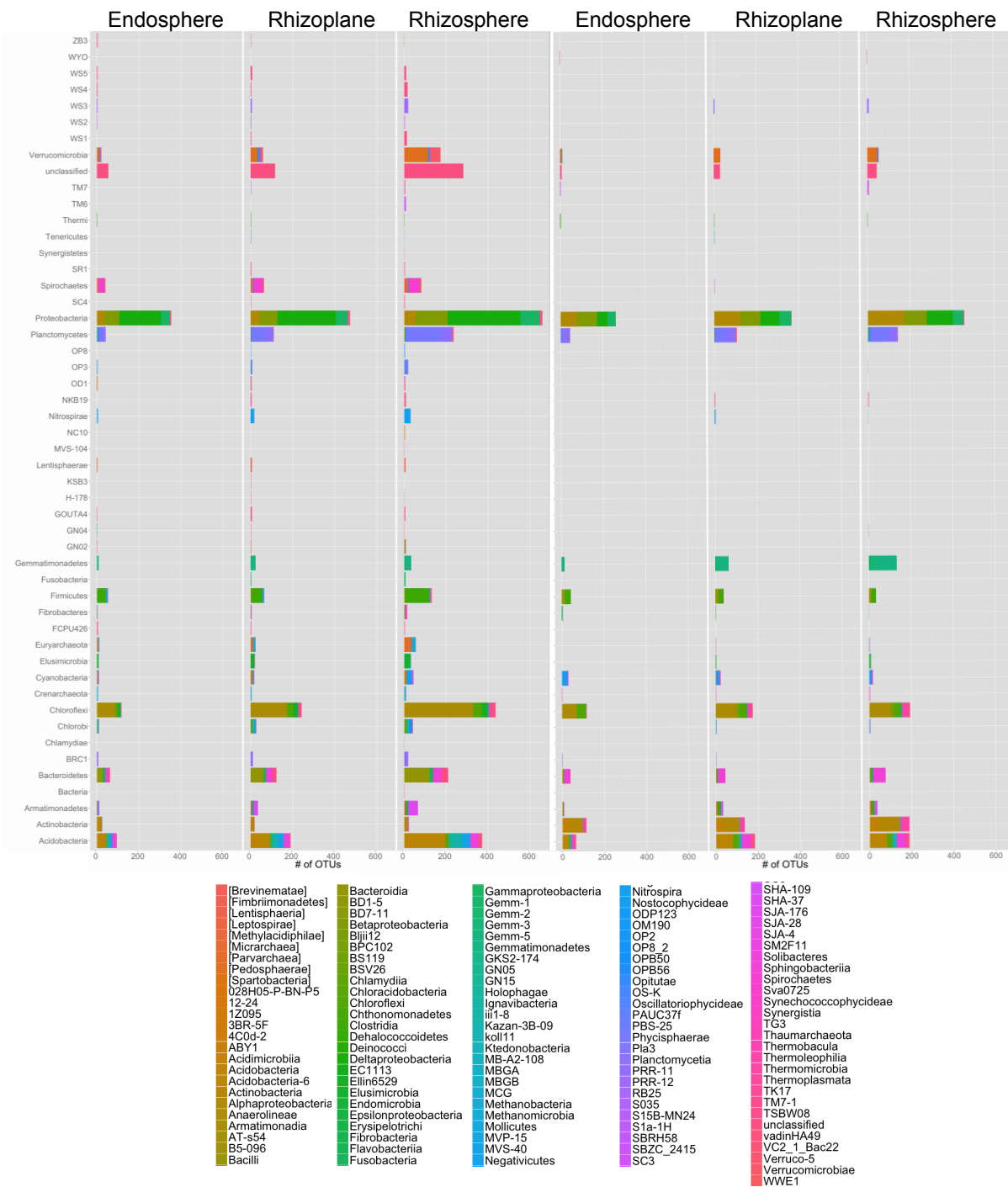
525

526

527

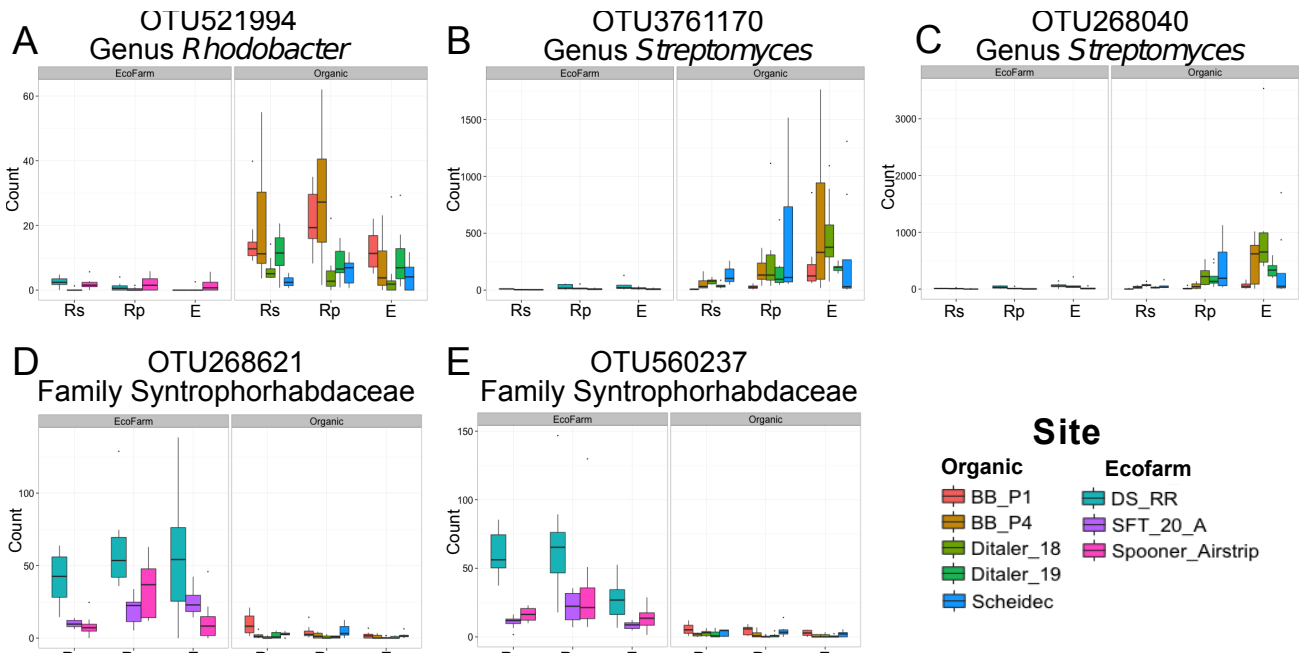
528

# Ecofarm Organic



529

530 **Fig. S20. OTUs that are significantly differentially abundant between cultivation practices**  
 531 **mainly vary within the phyla of Proteobacteria, Acidobacteria, Actinobacteria, and**  
 532 **Bacteroidetes.**



533

534 **Fig. S21. OTUs belonging to plant growth promoting rhizobacteria (PGPRs), methane**  
 535 **cycling bacteria, and antibiotic producing bacteria are differentially abundant under**  
 536 **different cultivation practices. (a – e) Counts for OTUs separated by compartment (x-axis)**  
 537 **and field site (color).**

538

539

540

541

542

543

544

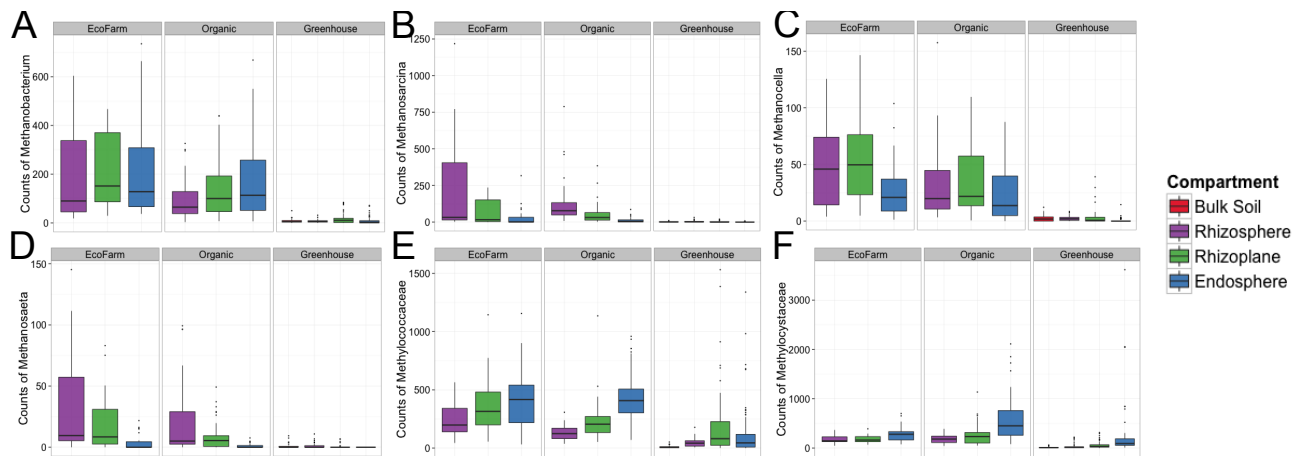
545

546

547

### Site

Organic	Ecofarm
BB_P1	DS_RR
BB_P4	SFT_20_A
Ditaler_18	Ditaler_19
Ditaler_19	Spooner_Airstrip
	Scheidec



548

549 **Fig. S22. OTUs involved in methane formation and oxidation have various patterns of**  
 550 **abundance across the different rhizocompartments and growth conditions. (a)** The sum of  
 551 the abundance of all OTUs within the methanogenic genus *Methanobacterium*. **(b)** The sum of  
 552 the abundance of all OTUs within them methanogenic genus *Methanosarcina*. **(c)** The sum of the  
 553 abundance of all OTUs within the methanogenic genus *Methanocella*. **(d)** The sum of the  
 554 abundance of all OTUs within the methanogenic genus *Methanosaeta*. **(e)** The sum of the  
 555 abundance of all OTUs within the methanotrophic family Methylococcaceae. **(f)** The sum of the  
 556 abundance of all OTUs within the methanotrophic family Methylocystaceae.

557

558

559

560

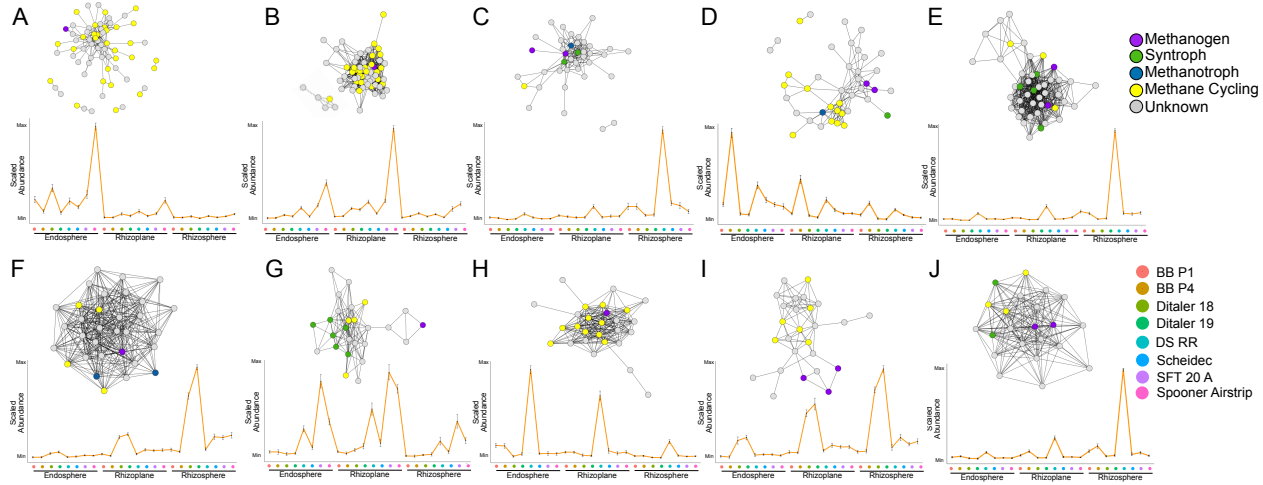
561

562

563

564

565



566

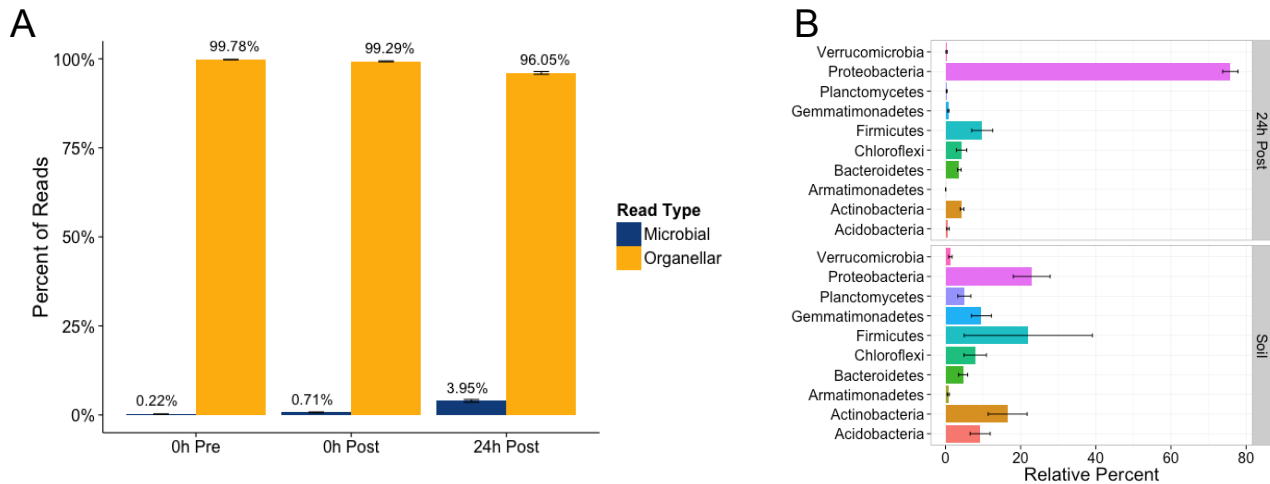
567 **Fig. S23. Modules of the co-abundance network associated with methane cycling.** Each  
 568 node represents an OTU and is colored by that OTUs presumed function in methane cycling. An  
 569 edge is drawn between OTUs if they have a Spearman correlation value of 0.6 or greater. **(a)**  
 570 Module 6 and the average abundance profile for OTUs within the module. **(b)** Module 17 and  
 571 the average abundance profile for OTUs within the module. **(c)** Module 53 and the average  
 572 abundance profile for OTUs within the module. **(d)** Module 58 and the average abundance  
 573 profile for OTUs within the module. **(e)** Module 75 and the average abundance profile for OTUs  
 574 within the module. **(f)** Module 152 and the average abundance profile for OTUs within the  
 575 module. **(g)** Module 184 and the average abundance profile for OTUs within the module. **(h)**  
 576 Module 191. **(i)** Module 205 and the average abundance profile for OTUs within the module. **(j)**  
 577 Module 252 and the average abundance profile for OTUs within the module. All error bars  
 578 represent standard error.

579

580

581

582

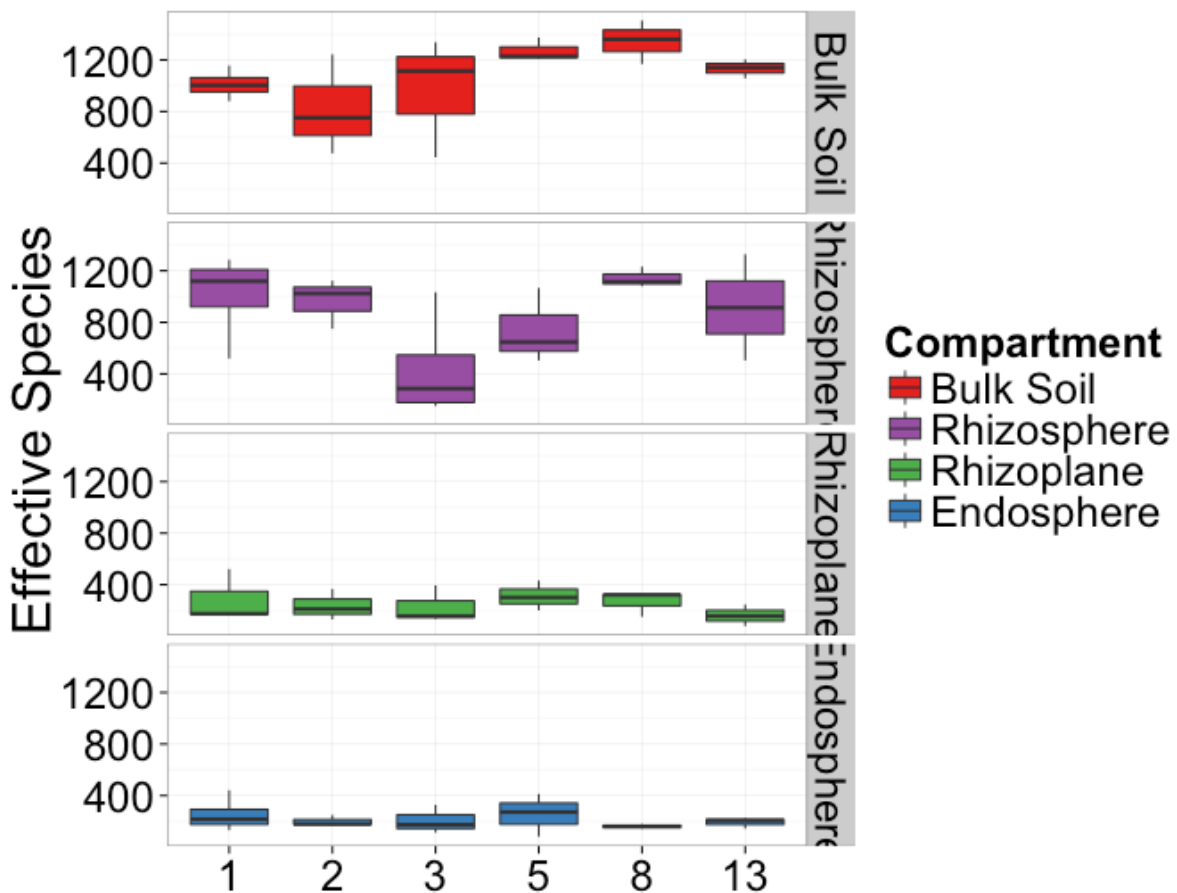


583

584 **Fig. S24 Microbe assembly into the endosphere at or before 24 hours is not a consequence**

585 **of carryover from soil contact.** (A) Microbe ratios in the interior of roots before transplantation  
 586 into soil, just after transplantation into soil, and after 24 hours in the soil. Mean percentages of  
 587 each read type are displayed above each bar. (B) Relative abundance of phyla between bulk soil  
 588 and 24 hours post transplantation into soil.

589



590

591 **Fig S25 Alpha diversity measurements of microbial communities in all compartments over**  
 592 **time.** Effective species =  $e^{\text{Shannon\_diversity}}$

593

594

595

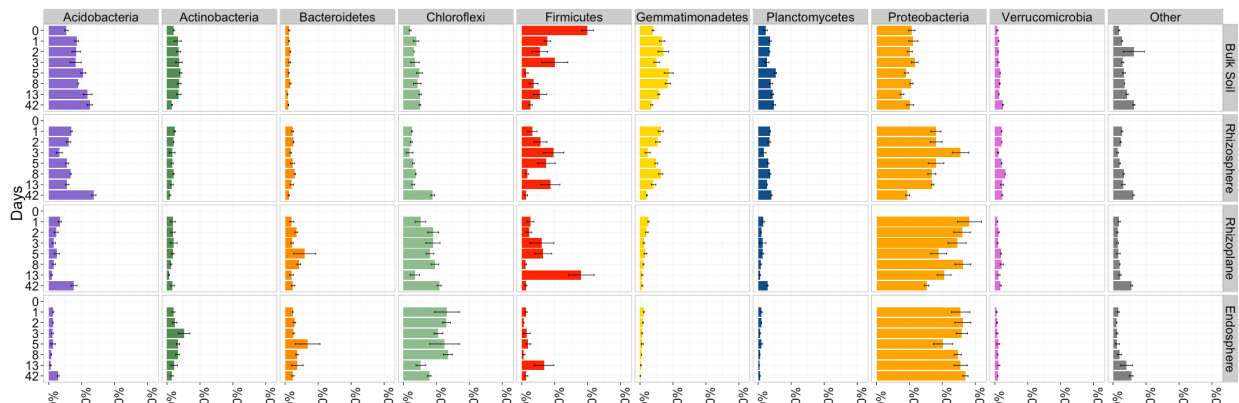
596

597

598

599

600



601  
602 **Fig. S26. There are slight shifts in the relative abundance of different phyla during the**  
603 **acquisition of root-associated microbiomes in each rhizocompartment.**

604

605

606

607

608

609

610

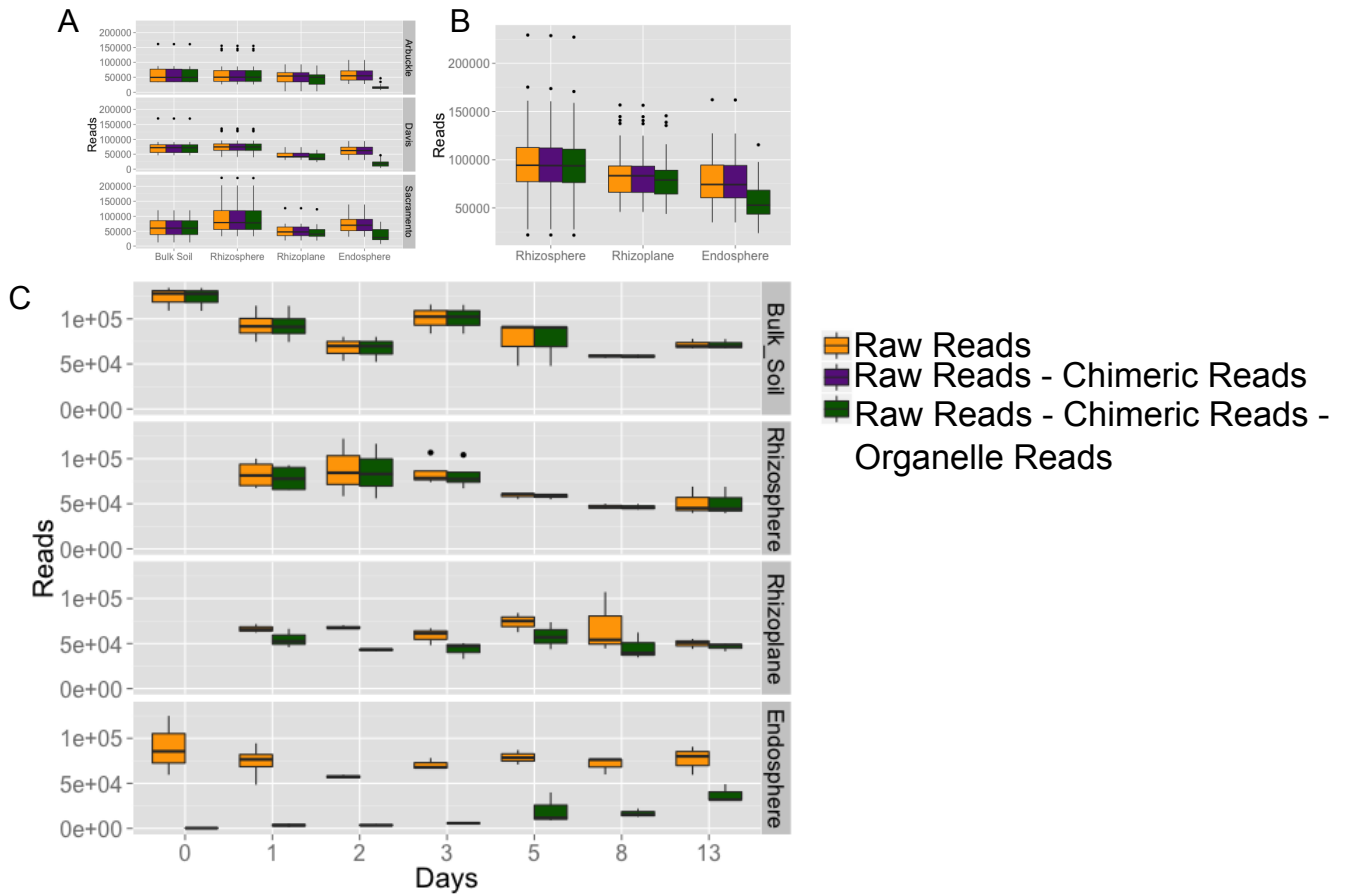
611

612

613

614

615



616

617 **Fig. S27 Sequencing effort for each rhizocompartment in each experiment.** (A) Greenhouse  
 618 experiment. (B) Field Experiment. (C) Time series experiment. Colors represent different points  
 619 in the sequence processing pipeline.

620

621

622

623

624

625

626

627

628

629 **Supplementary Dataset Legends**

630

631 **Dataset S1. Table showing number of replicates per factor in the greenhouse and field**  
632 **experiment.**

633

634 **Dataset S2. Table displaying sequencing effort for each sample in the greenhouse**  
635 **experiment.**

636

637 **Dataset S3. ANOVA results for how various factors affect alpha diversity in the**  
638 **greenhouse experiment.**

639

640 **Dataset S4. Pairwise comparisons of alpha diversities between each compartment in each**  
641 **soil of the greenhouse experiment.** Hypothesis testing was carried out using Wilcoxon rank  
642 sum tests and corrected for multiple testing using the Benjamini-Hochberg method.

643

644 **Dataset S5. Permutational MANOVA results using weighted and unweighted UniFrac as a**  
645 **distance metric for the greenhouse and field experiments.** (A) Weighted UniFrac on whole  
646 greenhouse data. (B) Weighted UniFrac on Greenhouse data subsetted to bulk soil and  
647 rhizosphere samples. (C) Weighted UniFrac on Greenhouse data subsetted to bulk soil and  
648 rhizoplane samples. (D) Weighted UniFrac on Greenhouse data subsetted to bulk soil and  
649 endosphere samples. (E) Weighted UniFrac on Greenhouse data subsetted Arbuckle samples. (F)  
650 Weighted UniFrac on Greenhouse data subsetted Sacramento samples. (G) Weighted UniFrac on  
651 Greenhouse data subsetted to Davis samples. (H) Unweighted UniFrac on whole greenhouse  
652 data. (I) Unweighted UniFrac on Greenhouse data subsetted to bulk soil and rhizosphere  
653 samples. (J) Unweighted UniFrac on Greenhouse data subsetted to bulk soil and rhizoplane  
654 samples. (K) Unweighted UniFrac on Greenhouse data subsetted to bulk soil and endosphere  
655 samples. (L) Unweighted UniFrac on Greenhouse data subsetted Arbuckle samples. (M)  
656 Unweighted UniFrac on Greenhouse data subsetted Sacramento samples. (N) Unweighted  
657 UniFrac on Greenhouse data subsetted to Davis samples. (O) Weighted UniFrac on whole Field  
658 Experiment data. (P) Unweighted UniFrac on whole Field Experiment data.

659  
660 **Dataset S6. Comparisons of phyla differential abundance between compartments in the**  
661 **greenhouse experiment.** Hypothesis testing was carried out using Wilcoxon rank sum tests and  
662 corrected for multiple testing using the Benjamini-Hochberg method.  
663  
664 **Dataset S7. OTUs that are significantly differentially abundant between**  
665 **rhizocompartments in the greenhouse experiment.**  
666  
667 **Dataset S8. Results of soil chemical analysis from the greenhouse experiment.**  
668  
669 **Dataset S9. OTUs that are significantly differentially abundant between**  
670 **rhizocompartments for each soil tested in the greenhouse experiment.**  
671  
672 **Dataset S10. GPS coordinate locations for all the rice fields where soil or plant material**  
673 **was collected.**  
674  
675 **Dataset S11. Pairwise comparisons of alpha diversities between each cultivar in each**  
676 **compartment in each soil.**  
677  
678 **Dataset S12. OTUs that are significantly differentially abundant in each cultivar of each**  
679 **rhizocompartment of each soil in the greenhouse experiment.**  
680  
681 **Dataset S13. Table displaying sequencing effort in the field experiment.**  
682  
683 **Dataset S14. Impacts of tested factors on alpha diversities in the field experiment.** ANOVA  
684 results are shown along with Wilcoxon rank sum tests between cultivation practices in each  
685 compartment.  
686  
687 **Dataset S15. Pairwise comparisons of alpha diversities between each compartment of each**  
688 **field site for the field experiment.** Hypothesis testing was carried out using Wilcoxon rank sum  
689 tests and corrected for multiple testing using the Benjamini-Hochberg method.

690  
691 **Dataset S16. Comparisons of phyla differential abundance between compartments in the**  
692 **greenhouse experiment.** Hypothesis testing was carried out using Wilcoxon rank sum tests and  
693 corrected for multiple testing using the Benjamini-Hochberg method.  
694  
695 **Dataset S17 OTUs that are significantly differentially abundant between the**  
696 **rhizocompartments in each field site tested of the field experiment.**  
697  
698 **Dataset S18 OTUs that are significantly differentially abundant between cultivation**  
699 **practices in each rhizocompartment of the field experiment.**  
700  
701 **Dataset S19. Taxonomies that belong to clones of *mcrA* sequenced from the rhizosphere**  
702 **and endosphere of plants grown in the DS RR field.**  
703  
704 **Dataset S20. OTUs in the co-abundance network and the modules they are assigned to.**  
705  
706 **Dataset S21. OTUs modules containing methanogenic archaea.** OTUs are labeled for their  
707 known relationships to methane cycling.  
708  
709 **Dataset S22. Taxonomies significantly enriched (FDR <= 0.05) in OTU network modules**  
710 **containing the methanogenic archaea genera *Methanobacterium*, *Methanosarcina*,**  
711 ***Methanocella*, and *Methanosaeta*.**  
712  
713 **Dataset S23. Taxonomies significantly enriched (FDR <= 0.05) in OTU network modules**  
714 **containing the methanogenic archaea genera *Methanobacterium*, *Methanosarcina*,**  
715 ***Methanocella*, and *Methanosaeta*.**  
716  
717 **Dataset S24. Comparisons of phyla differential abundance between compartments in the**  
718 **timecourse experiment.** Hypothesis testing was carried out using Wilcoxon rank sum tests and  
719 corrected for multiple testing using the Benjamini-Hochberg method.  
720

721   **Dataset S25** Sequencing primers used to amplify the 16S rRNA gene.